

THE MAGNETIC EFFECT OF ANNEALING NICKEL-IRON
ALLOYS UNDER TENSION

by

Edward A. Gaugler

Thesis submitted to the Faculty of the Graduate School
of the University of Maryland in partial
fulfillment of the requirements for the
degree of Doctor of Philosophy

1950

UMI Number: DP70358

All rights reserved

INFORMATION TO ALL USERS

The quality of this reproduction is dependent upon the quality of the copy submitted.

In the unlikely event that the author did not send a complete manuscript and there are missing pages, these will be noted. Also, if material had to be removed, a note will indicate the deletion.



UMI DP70358

Published by ProQuest LLC (2015). Copyright in the Dissertation held by the Author.

Microform Edition © ProQuest LLC.

All rights reserved. This work is protected against unauthorized copying under Title 17, United States Code



ProQuest LLC.
789 East Eisenhower Parkway
P.O. Box 1346
Ann Arbor, MI 48106 - 1346

ACKNOWLEDGMENT

I wish to thank Dr. J. H. McMillen, Professor of Physics, and Dr. L. R. Maxwell, Chief of the Solid State Subdivision of the Naval Ordnance Laboratory, who were co-directors of this problem, for their assistance and their valuable suggestions. I am indebted to Dr. G. W. Elzen, with whom the writer has been associated for a number of years, for many valuable discussions in this field. I appreciate the assistance of the personnel of the Magnetic Materials Subdivision of the Naval Ordnance Laboratory in obtaining these data.

TABLE OF CONTENTS

INTRODUCTION

	Page
SECTION I	
PREPARATION OF MATERIALS	1
1. Melting	1
2. Rolling	4
3. First Hydrogen Anneal	7
4. Tension Anneal	12
5. Magnetic Anneal	16
SECTION II	
MAGNETIC MEASUREMENTS	18
1. Permeability	18
2. Anisotropy	24
SECTION III	
RESULTS OF TENSION ANNEALING	28
SECTION IV	
INTERPRETATION OF RESULTS	36
1. Case I - Anisotropic Magnetostriction	43
2. Case II - Isotropic Magnetostriction	44
3. Magnetization Process	45
SECTION V	
THE PERMALLOY PROBLEM	48
SECTION VI	
MAGNETIC ANNEALING	53

TABLE OF CONTENTS (Cont'd)

SECTION VII	Page
SUPERSTRUCTURE	62
SECTION VIII	
BIBLIOGRAPHY OF LITERATURE CITED	66

LIST OF TABLES

Table		Page
1	Chemical Analysis of Raw Materials	2
2	Chemical Analysis of Ingots	5
3	Effect of Magnetic Annealing of Iron	61

LIST OF PLATES

Plate		Page
1	Hydrogen Purification System	9
2	Test Specimens used in Tension Annealing	13
3	Mechanical Suspension used in Tension Annealing..	14
4	Furnace Assembly used in Tension Annealing	15
5	Relation between Intrinsic and Apparent Permeability of a Cylindrical Rod	19
6	Free Body Diagram of Curved Portion of Tension Specimen	21
7	Magnetic Dynamometer	25
8	Maximum Permeability vs Composition for Tension Annealing	29
9	Maximum Permeability vs Tension used in Tension Annealing (40-55% Ni)	31
10	Maximum Permeability vs Tension used in Tension Annealing (57.5 - 65% Ni)	32
11	Maximum Permeability vs Tension used in Tension Annealing (67.5 - 77.5% Ni)	33
12	Maximum Permeability vs Tension used in Tension Annealing (80 - 85% Ni)	34
13	Maximum Permeability vs Tension used in Tension Annealing (90 - 100% Ni)	35
14	Saturation Magnetostriction of Polycrystalline Ni-Fe Alloys	37
15	Saturation Magnetostriction of Single Crystal Ni-Fe Alloys for Two Principal Crystallographic Directions	39
16	Cubic Anisotropy Constant, K_1 , for Ni-Fe Alloys..	41
17	Effect of Cooling Rate on Ni-Fe Alloys	50

LIST OF PLATES (Cont'd)

Plate		Page
18	Effect on Maximum Permeability of Magnetic Annealing of Ni-Fe Alloys (85°C/hr.)	54
19	Effect on Maximum Permeability of Magnetic Annealing of Ni-Fe Alloys (15°C/hr.)	56
20	Anisotropy Introduced by Magnetic Annealing of Ni-Fe Alloys	58
21	Comparison of Resistivity of Annealed Ni-Fe Alloys Showing Presence of Superstructure	63
22	Maximum Permeability of Baked Nickel-Iron Alloys	64

LIST OF SYMBOLS

B	Magnetic Induction
H	Magnetizing Force
μ	Permeability
η	Coefficient of Static Friction
T	Tensile Stress
θ, ψ	Angle Variables
f_k	Energy Density due to Cubic Anisotropy
f_{mc}	Energy Density due to Magnetostriction
f_{MK}	Anisotropy Energy Density introduced by Magnetic Annealing
$\lambda_{100}, \lambda_{111}$	Saturation Magnetostriction Coefficients along the $[100]$ and $[111]$ Crystallographic Directions
$\bar{\lambda}$	Saturation Magnetostriction Constant for Polycrystalline Materials
λ	LaGrange's Undetermined Multiplier
K_1	Cubic Anisotropy Coefficient
K_0	Anisotropy Coefficient introduced by Magnetic Annealing
P_{ik}	Component of Tensile Stress
α_i, γ_i	Direction Cosines with respect to Crystallographic Axes of Magnetization and Tensile Stress respectively
I_s	Saturation Magnetic Intensity
E	Modulus of Elasticity
G	Shear Modulus of Elasticity
ϵ	Elastic Displacement
σ	Poisson's Ratio

INTRODUCTION

The magnetic properties of nickel-iron alloys containing 50% to 90% nickel are radically affected by heat treatment. It is well known that rapid cooling below the magnetic transformation temperature produces a maximum permeability at 78.5% nickel. Also it has been shown that slow cooling in a magnetic field yields a maximum permeability at 68% nickel. Although these characteristics have been known for some time, the mechanism involved is not well understood. (1)

The magnetic characteristics of some of these alloys under strain at ambient temperatures have been investigated. To the author's knowledge, no systematic investigation has been made on the effects of annealing these alloys under tension. Besides the purely theoretical interest in this problem, a knowledge of the effects due to tension annealing is important in the technology of processing magnetic materials. Consequently an investigation of tension annealing of this nickel-iron series was undertaken.

Certain magnetic properties of the nickel-iron alloys such as permeability, coercive force and remanence are extremely structure sensitive. To obtain consistent experimental data every stage in their processing from melting to final heat treatment must be exactly duplicated. Even apparently trivial differences in annealing boxes, melting furnaces, and gas atmosphere purifiers affect these sensitive

properties to some extent. For this reason well-known experiments on rate of cooling, and cooling in a magnetic field were carried out for the same alloys used in this tension annealing investigation. Only in this way could an accurate comparison be made between tension and standard methods of annealing.

SECTION I

PREPARATION OF MATERIALS

1. Melting. Alloys were prepared in 5% steps between 40 and 100% nickel. Additional alloys were later prepared in regions that appeared to be of special interest. The alloys were prepared by melting together electrolytic iron, electrolytic nickel, and electrolytic manganese in an induction furnace under carefully controlled conditions. This included melting the constituent metals under a vacuum and subsequently refining the melt in an atmosphere of hydrogen. Table 1 shows the purity of the raw materials used in the preparation of these alloys.

The furnace used for melting was an Ajax pressure-vacuum furnace of 30 lb. melting capacity. Power for melting was furnished by a 3000 cycle, 50 KW M-G set.

The charge, consisting of iron, nickel, and manganese in each case weighed a total of 9000 gms. Iron and nickel made up the bulk of the charge. These were loaded in a crucible of high purity electrically fused MgO, free from sulfur. A small amount of manganese (0.5%) was added to facilitate hot working. It was placed in an externally operated chute, making it possible to make a manganese addition at the desired time. This was necessary to prevent the loss of the entire amount of manganese, because of its relatively high vapor pressure.

TABLE 1.

CHEMICAL ANALYSIS OF RAW MATERIALS

<u>METAL</u>	<u>Fe</u>	<u>Ni</u>	<u>Mn</u>	<u>Si</u>	<u>P</u>	<u>S</u>	<u>C</u>	<u>Co</u>	<u>Cu</u>	<u>Cr</u>	<u>Mo</u>	<u>W</u>	<u>V</u>	<u>Al</u>	<u>Sb</u>
** Fe	99.97	Tr.	nil	0.01	0.005	0.006	0.014*	nil	-	Tr.	nil	-	nil	nil	-
** Ni	0.07	99.22	-	0.009	0.002	0.018	0.013*	0.59	0.005	-	0.001	-	-	-	0.004
** Mn	0.003	-	99.95	0.005	0.004	0.015	0.02	-	0.001	-	0.001	-	-	0.004	-

* Determined with Leco Carbon Determinator

** Electrolytic

After properly loading the charge, the furnace chamber was secured and evacuated until a pressure of 0.5 to 0.6 mm was attained, as measured on a Stokes McLeod gauge. The power was then turned on and adjusted to 10 KW for a period of five minutes, and raised, thereafter in steps of 2 KW every five minutes until complete melting occurred, at approximately 26 KW. The gradual heating cycle was adopted to prolong the life of the crucibles which are quite susceptible to heat shock. Evacuation of the furnace was continued during this time. The cycle lasted for about forty-five minutes to an hour. Dissolved gases were evolved from the metal during the melting period, so that the final pressure over the molten alloy rose to a somewhat higher value, ranging from 1.0 to 2.5 mm. Some of the carbon and oxygen present in the metal were no doubt removed as CO during this preliminary melt-down in a vacuum.

Further refinement of the melt was carried out by the use of a hydrogen atmosphere. Pure dry hydrogen was allowed to fill the evacuated chamber. Wet hydrogen, prepared by passing hydrogen directly from the tank over water, was then allowed to flow at the rate of 8 c.f.h. for 1/2 hour. After this decarburizing treatment, deoxidation was effected by substituting pure dry hydrogen (dew point -92°F) for the wet hydrogen at the same rate of flow, for an additional one-half hour.

Although from a purification standpoint it is desirable to pour the melt under a pure dry hydrogen atmosphere, this would result in a porous ingot, due to evolution of the dissolved hydrogen during the freezing process. It is preferable to flush out the hydrogen and replace it by helium just prior to pouring because the latter gas is relatively insoluble. Since it is desirable to add manganese at this time, the two operations are done together.

The chamber was first flushed with pure dry helium, in order to remove the hydrogen safely. The manganese addition was made at this time to allow sufficient time for mixing, and the chamber again evacuated to reduce more completely the dissolved gases. The evacuation proceeded until a pressure of 5 mm was reached, at which time the chamber was again filled with pure helium. The temperature of the melt was finally adjusted to 1540°C , as determined with an optical pyrometer, and the alloy was chill cast in a cast iron mold coated with alundum cement. The resulting ingots were square in cross section and of a tapered type with big end up, measuring $3\frac{1}{2}$ inches at the top and $2\frac{3}{4}$ inches at the bottom, and about $6\frac{1}{2}$ inches in length.

The final composition and purity of the series of Fe-Ni alloys prepared by this method may be judged from Table 2.

2. Rolling. Since all nickel-iron alloys were cast in square ingots it was necessary to cut slabs of 1" thickness from these ingots in order to be able to roll them on our laboratory type 2-high rolling mill which has 6" diameter

TABLE 2.
 CHEMICAL ANALYSIS OF INGOTS
 (In Percent)

NICKEL (Nominal)	<u>Ni</u>	<u>Fe</u>	<u>Mn</u>	<u>Co</u>	<u>C</u> *	<u>Si</u>	<u>S</u>	<u>P</u>	<u>Cu</u>
40	39.52	59.67	0.55	0.25	0.006	0.001	0.004	0.002	0.002
45	44.69	54.50	0.52	0.28	-	0.001	0.003	0.002	0.002
50	49.61	49.53	0.53	0.32	-	0.001	0.004	0.001	0.002
55	54.61	44.48	0.55	0.35	-	0.001	0.004	0.001	0.002
57.5	57.81	41.29	0.53	0.36	-	0.001	0.004	0.001	0.002
60	59.63	39.43	0.55	0.38	0.005	0.001	0.004	0.001	0.002
62.5	62.41	36.67	0.51	0.40	-	0.001	0.004	0.001	0.003
65	64.41	34.54	0.63	0.41	0.004	0.001	0.004	0.001	0.003
67.5	67.34	31.71	0.51	0.43	0.003	0.001	0.004	0.001	0.003
70	69.25	29.66	0.64	0.44	0.004	0.001	0.004	0.001	0.003
75	74.23	24.71	0.57	0.48	0.005	0.001	0.003	0.001	0.003
77.5	77.13	21.82	0.55	0.49	-	0.001	0.003	0.001	0.003
80	79.56	19.36	0.56	0.51	-	0.001	0.003	0.001	0.003
81	81.04	17.94	0.50	0.51	-	0.001	0.003	0.001	0.003
82.5	82.04	16.86	0.57	0.52	0.005	0.001	0.002	0.001	0.003
85	84.57	14.43	0.45	0.54	-	0.001	0.002	0.001	0.003
90	89.47	9.40	0.55	0.57	-	0.001	0.002	0.001	0.004
95	94.13	4.68	0.58	0.60	-	0.001	0.001	0.001	0.004
100	98.87	0.025	0.46	0.63	0.005	0.001	0.001	0.001	0.004

* Determined with Leco Carbon Determinator

NOTE: After final heat treatment, the sulfur and carbon content will be substantially reduced.

rolls with 10" face and a maximum opening of only 1-inch. These slabs were cross sectional pieces cut transverse to direction of casting. They were machined on all surfaces to remove scale and surface impurities that may have been picked up from the molds during the casting process. At this stage the machined pieces had dimensions of approximately 3 1/4" wide by 3 1/4" long by 1" thick.

This piece was then heated at 1200°C in an electrical furnace, and this temperature was held for forty-five minutes to insure uniform temperature throughout the slab. A small flow of helium was passed into the heating chamber to reduce oxidation of the slab during heating operations. Initial hot rolling consisted of taking four passes at .005" per pass on the 2-high mill and then reheating for five minutes before repeating the operation. This cycle was repeated until the cast dendritic structure had been broken down and then it was possible to take four passes at .015" per pass for a total of .060" reduction in thickness before reheating. This practice was repeated until the thickness of the slab had been reduced to .250" thus giving a total hot reduction of 75%.

The slab was then pressed flat on the 200 ton hydraulic press and placed in the furnace for 30 minutes at 1200°C before air cooling. All edges were machined for removal of edge cracks and all surfaces were sandblasted in order to remove the scale that had formed during hot rolling operations. At this stage the measurements of the piece were approximately .250" thick x 3 1/4" wide x 10" long.

The slab was then cold rolled from .250" down to .023" thickness taking alternate passes of .007" and .008" reduction per pass, thus giving a total cold reduction for this stage of 91%. The material was then coiled and given a pot anneal in hydrogen atmosphere for one hour at 950° C and furnace cooled.

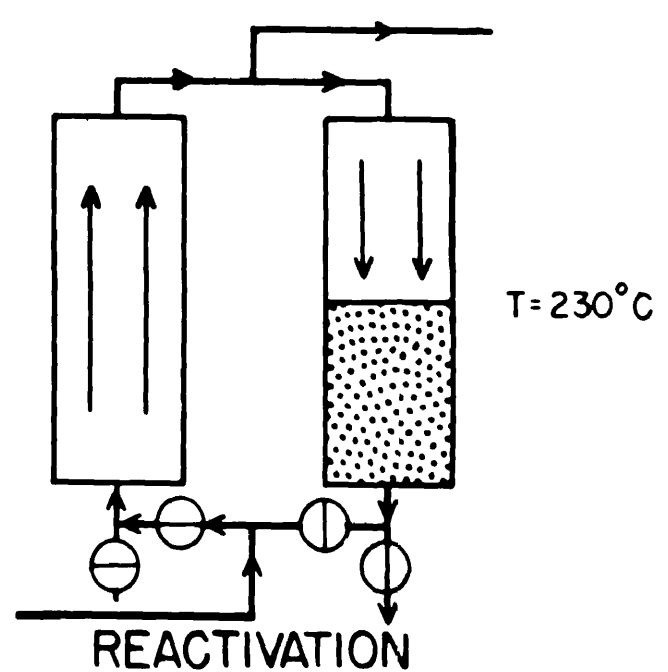
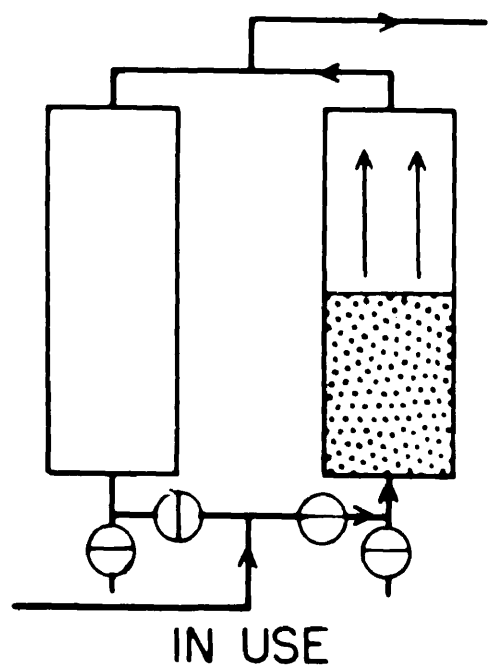
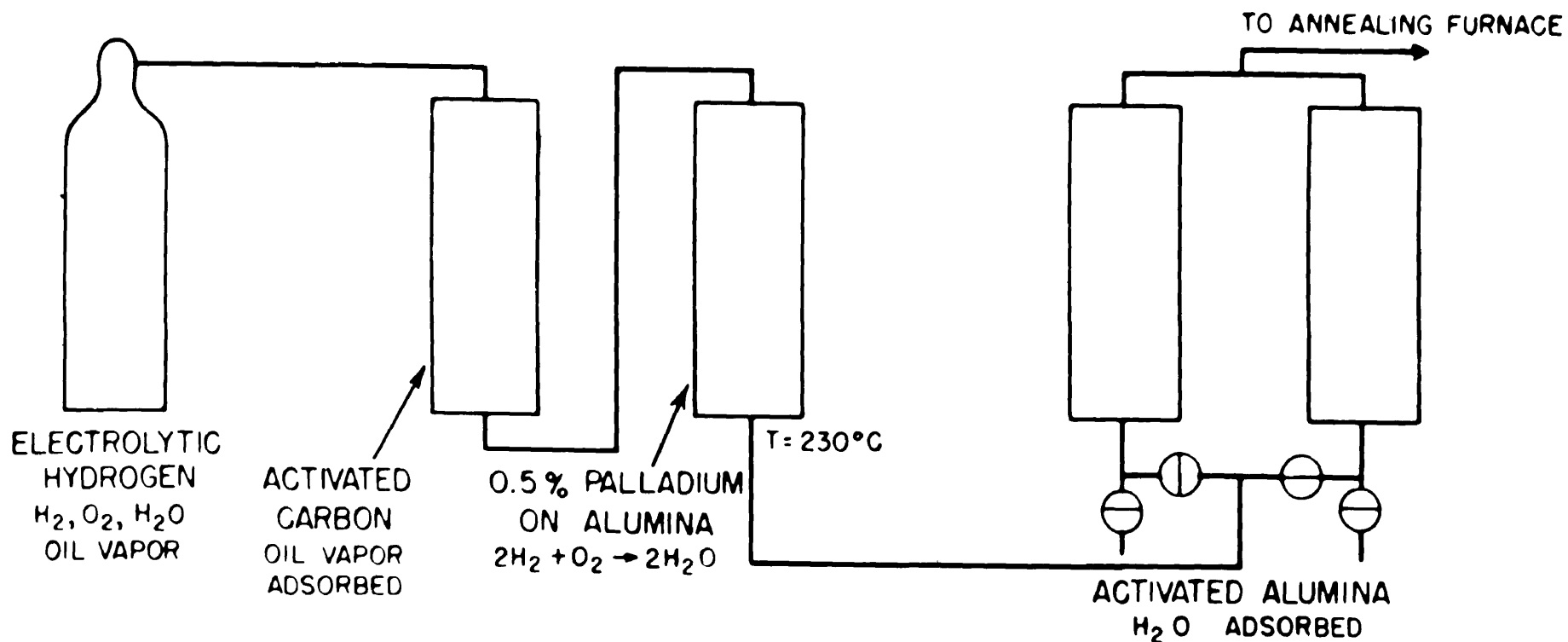
Further cold rolling was done by taking reductions of only .001" to .003" per pass until a thickness of .014" had been reached, thus giving a total cold reduction of 40% after anneal. The material was then ready for stamping into laminations or cutting into test specimens, as required, before it received the final hydrogen anneal.

3. First Hydrogen Anneal. It is well known that superior results can be obtained by annealing soft magnetic materials at a relatively high temperature in a pure dry hydrogen atmosphere. Under these conditions not only is oxidation prevented, but impurities are actually removed from the charge. Some materials, such as the nickel-iron alloys, are particularly susceptible to very small impurities in the annealing atmosphere. Although commercial hydrogen can be obtained at 99.5 percent purity, such hydrogen is not satisfactory for magnetic work and must be further purified.

Commercial hydrogen is produced by several processes, but electrolytic hydrogen is preferred. Although its total purity may be lower than that obtained by other processes, electrolytic gas is preferred because the impurities are

mainly oxygen and water vapor, both of which can be readily removed.

Plate 1 is a schematic diagram of the hydrogen purification system which was developed for the purpose. As indicated, the electrolytic hydrogen consists mainly of hydrogen, oxygen, and water vapor. Because the gas is oil-pumped, small traces of oil vapor may also be present. Since the oxygen is burned over a palladium catalyst the activity of which may be readily impaired by the presence of oil vapor, the gas is first passed through a tower containing activated charcoal which removes oil and other vapors that might "poison" the catalytic action. The catalyst consists of one-half percent palladium-on-alumina pellets. Although satisfactory results can be achieved at room temperatures, the catalyst is actually maintained at 230°C. It is reported that a greater portion of the surface area of the catalyst is active at the higher temperature, and it is less susceptible to poisoning. Because the catalyst is maintained above the temperature of the normal boiling point of water, inactivity due to the possibility of water condensation on its surface is minimized. It is reported that by this method the oxygen content is reduced below one part per million. The oxygen content was checked using calorimeter techniques and shown to be less than one part per hundred thousand. Keeping the catalyst at a high temperature is an efficient method for removing oxygen and should operate indefinitely free from maintenance.



At this point only water is left to be removed. This removal is accomplished by adsorption on activated alumina. Activated alumina is aluminum oxide whose specific surface has been greatly increased. Gases, the normal boiling points of which are relatively high, will condense on its surface. In the case of water vapor, activated alumina will adsorb at substantially 100 percent efficiency at room temperature until 12 to 14 percent of its dry weight of moisture has been adsorbed. Thus adsorption occurs in layers proceeding from the entrance end of the moist gas towards the exit end. Since the exit end is substantially free from adsorbed water, the exit gas is very dry.

Activated alumina is available in many grades. We have chosen grade P1, which is pure alumina, because of its higher reactivation temperature, and because practically all published data pertain to this particular grade. Based on calculations involving total gas flow and the amounts of impurities present, the unit is reactivated before the moist zone reaches the exit end. By the valve connections indicated, the gas is then dried through the other tower, and a portion of this pure dry gas is used for reactivation. It should be noticed that the reactivating gas flows opposite to that being dried and in this way the moist zone is forced back out the same way that it came. Thus, if the reactivation is incomplete the residual moisture is located in the moist end of the dryer. The dry end should never be per-

mitted to become moist. It is surprising that in many of the commercial units the reactivating gas flows in the same direction as the gas being dried. In that case, during reactivation, the moisture is forced out through the dry zone. If it is incomplete, the gas being dried is contaminated due to the residual moisture left in the exit end. Another feature of this drying system is that pure dry hydrogen is used for reactivation. Thus the adsorbant is never exposed to air or disconnected from the system. If the maximum reactivation temperature is never exceeded, this drying system should operate indefinitely and substantially free from maintenance.

Special precautions are taken to eliminate air leaks in the system. Packless valves are used throughout. Soldered joints and lead gasket seals are employed. Elimination of air leaks is particularly important since the performance of the system is usually checked by measurement of its total moisture content (by dewpoint) and air leaks occurring after the deoxidation tower might be noticed. Metal hose is used for all flexible gas connections. Organic tubing in general is not satisfactory due to its absorption of water. Such adsorption is particularly bad if the hose is used intermittently, as in dew point determinations.

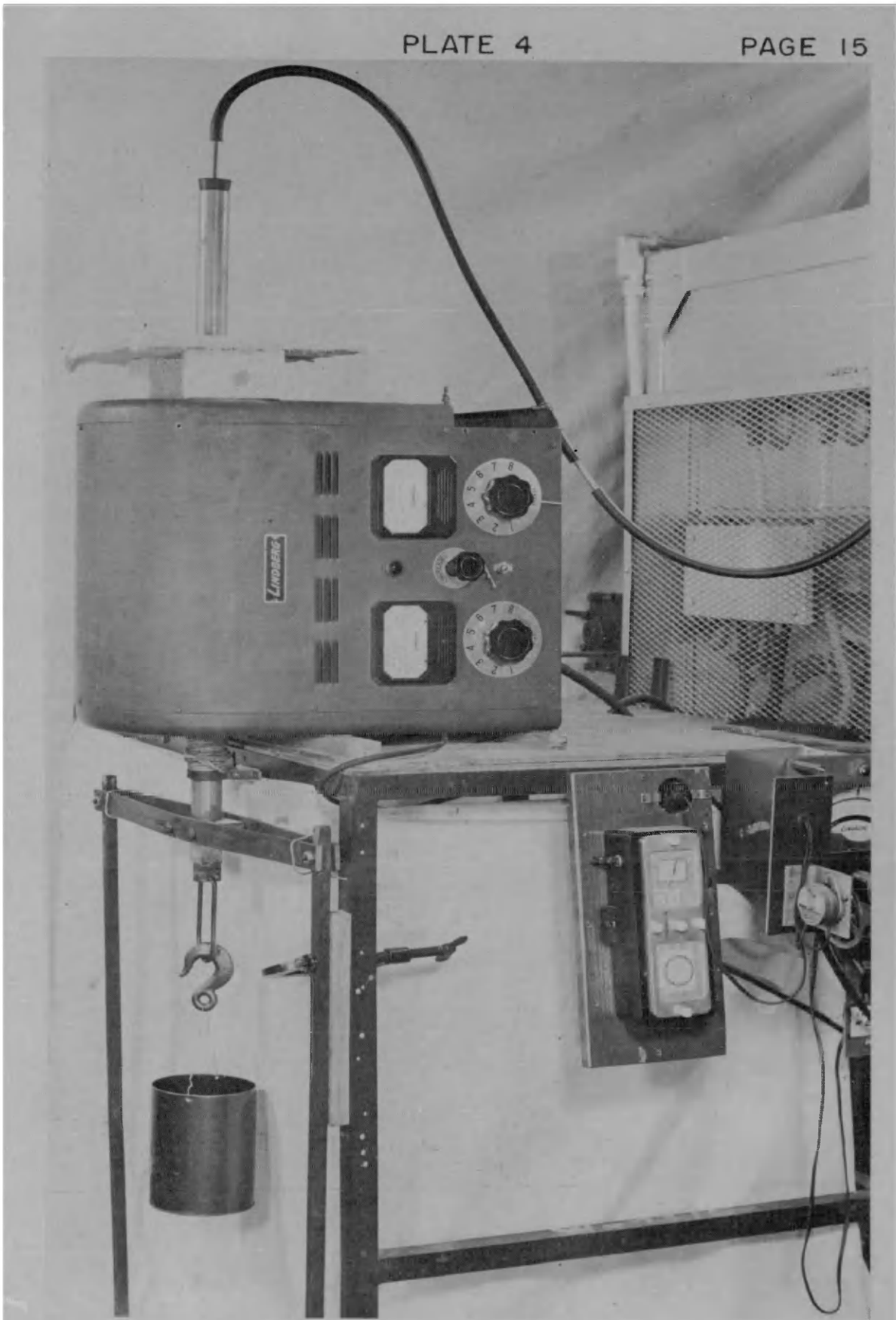
The moisture content of the purified gas as measured by dew point determinations is consistently below -90° F. The oxygen content is less than one part per hundred thousand.

The mere introduction of pure dry hydrogen into the furnace is not sufficient to insure a pure atmosphere within the furnace. Although the charge is enclosed in a gas-tight metal container, gas will be evolved by the container during the anneal and in this way contaminate the atmosphere. It has been found, however, that by using a suitable inner metal liner that is outgassed at a higher temperature than is intended for use, good and consistent results can be obtained thereafter.

One indication of the condition inside the furnace can be obtained from the dew point of the exit gas. If all the necessary precautions are taken, exit dew points of below -75°F can be obtained. Under such conditions maximum permeabilities of 270,000 can be consistently obtained in some of the commercial grades of high nickel-iron alloys. If pure dry hydrogen is used but the precaution of outgassing the container is not taken, a permeability of around 130,000 is obtained.

The annealing cycle used for the nickel-iron series was to hold the alloys for 18-hours at 1200°C , furnace cool to 1050°C and hold for four hours and furnace cool to room temperature. Subsequent annealing is described below.

4. Tension Anneal. A standard specimen used in tension annealing experiments is shown on the left of Plate 2. Plate 3 shows how the specimen was supported during the tension anneal. This assembly was inserted in the tube furnace, shown in Plate 4, containing a pure dry hydrogen atmosphere.



FURNACE ASSEMBLY
USED IN TENSION ANNEALING

Suitable weights were placed in the container at the bottom of Plate 4 to provide the necessary tension on the specimen. In order to prevent fusing of the specimen to its suspension, metal to metal contacts were prevented through isolation by refractories.

The annealing cycle employed in most cases had for its initial step the raising of the furnace slowly to 600° C where the temperature was maintained for one hour. The weight was then applied and the specimen was cooled at 80° C per hour down to 250° C. The tension was removed and the specimen withdrawn from the furnace. The cooling rate was controlled automatically by means of a standard on-off temperature controller driven by a special timing motor, (Plate 4, lower right).

5. Magnetic Anneal. In general, the specimens used in magnetic annealing experiments were annular ring specimens and circular discs. These specimens were mounted in special furnaces in which magnetic fields could be applied in preferred directions. For ring specimens, a circular field was generated by passing an electric current along the axis of a rod of circular cross-section. The rings were concentrically supported on this rod. In the case of discs, it was desired to generate a magnetic field parallel to a preferred diameter in the plane of each disc. The discs were annealed in a tube furnace centrally located on the axis of a water-cooled solenoid.

In order to prevent contamination, magnetic annealing was done in a pure dry hydrogen atmosphere. The furnace temperature was slowly raised to 600°C. This temperature was above the Curie temperature of all alloys in this series. The magnetic field was then turned on and the temperature maintained long enough to insure thermal equilibrium. The actual times used are indicated in the data to follow. The furnaces were then cooled at standardized cooling rates in the magnetic fields. The fields were not removed until the temperature dropped below 250°C.

The magnitude of the magnetic fields used was standardized and depended on the shape of the specimen. According to previous experience of the author, 87 oersteds was satisfactory for ring specimens. Due to large demagnetizing effects of the disc specimens, an applied field of approximately 1000 oersteds was used. This was sufficiently large to insure an internal field in excess of 87 oersteds.

SECTION II

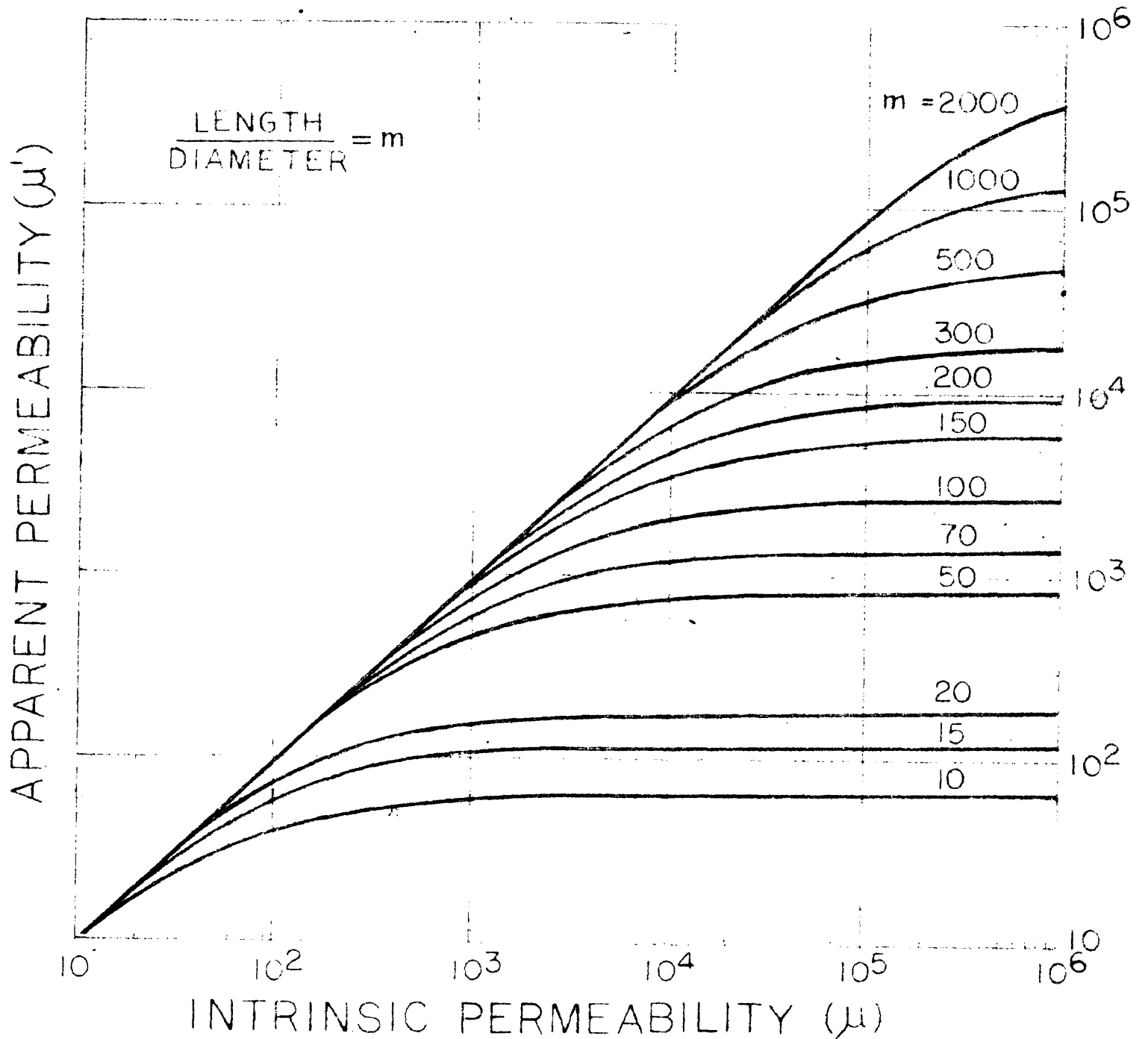
MAGNETIC MEASUREMENTS

1. Permeability. It is well known that the use of continuous ring specimens is preferred for high permeability measurements. The elimination of air gaps is essential in order to determine accurately the magnetizing force within the specimen. Because a constant magnetic potential is applied to the test sample, the magnetizing force will vary along the ring diameter. Therefore, it is desirable to keep the annular width of the ring small compared to its mean diameter. A satisfactory specimen for this type of investigation consisted of several rings, 1.625" i.d. by 2.00" o.d. and .011" thick. Such specimens were used throughout the investigation unless otherwise noted.

Unfortunately, it is difficult to apply a uniform tension on a ring specimen and therefore they were not used in tension annealing experiments. One method of introducing uniform tension during annealing would be to apply a known weight at the end of a straight magnetic specimen. Due to demagnetizing effects caused by the ends of this specimen, the intrinsic magnetic permeability cannot be determined accurately for high permeability alloys. One could use a wire whose length is large compared to its diameter. Plate 5 shows the relation between the intrinsic and apparent per-

PLATE 5
RELATION BETWEEN
INTRINSIC AND APPARENT PERMEABILITY
OF A CYLINDRICAL ROD

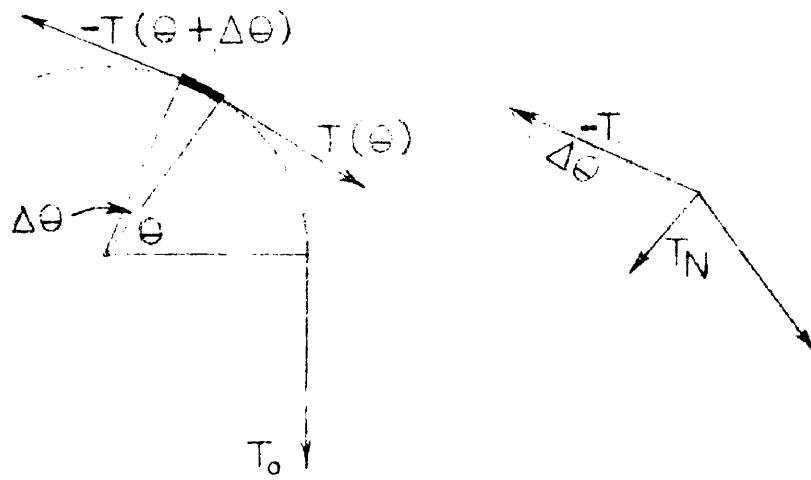
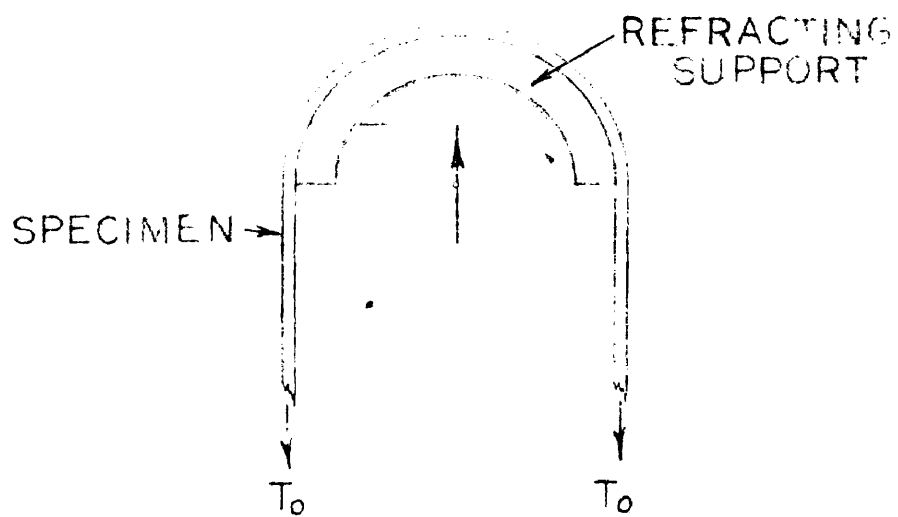
FROM BOZORTH, R. M. AND CHAPIN, D. M.
J.A.P. VOL. 13, 5, 320-326 MAY 1942



meability of a cylindrical rod as a function of its dimensional ratio, m , the ratio of length to diameter. It is seen that to measure an intrinsic permeability of one million a dimensional ratio in excess of 1000:1 is required. The problem of properly handling a number of such specimens would be difficult and the final results inconclusive. Therefore it was decided to employ a continuous specimen of the type shown in Plate 2. Overall dimensions are $4 \frac{5}{16}$ " long by $\frac{3}{4}$ " wide, and $\frac{1}{2}$ " high. This was fabricated using a single turn of tape, $9 \frac{5}{8}$ " long by $\frac{1}{2}$ " wide, and $.014$ " thick. A double lap joint was employed to minimize any demagnetizing effects caused by the joint. At the high temperature employed in the first hydrogen anneal, adjacent metallic surfaces in the joint fused together making its reluctance extremely low. The reluctance of this type of joint was checked by magnetic annealing a circular specimen. The permeability obtained was sufficiently high to prove that the reluctance of this joint was negligible for the tension annealing investigations.

One objection to this type of specimen is that the tension is not constant throughout its length. It is evident from consideration of the free body diagram shown in Plate 6 that static friction will reduce the tension in the curved portion of this specimen. An estimate of the minimum tension, T_{min} , found in the curved section was sought. The tension along an incremental element of the curve may be

PLATE 6
FREE BODY DIAGRAM
OF CURVED PORTION
OF TENSION SPECIMEN



represented by a Taylor series:

$$T(\theta + \Delta\theta) = T(\theta) + \frac{dT}{d\theta} \Delta\theta + \frac{1}{2!} \frac{d^2T}{d\theta^2} \Delta\theta^2 + \dots$$

The normal stress component on the curved support is $T\Delta\theta$.

Due to friction this changes the tension by an amount

$$\Delta T = -\eta T \Delta\theta$$

where η is the static coefficient of friction. Equating

and passing to the limit, $\Delta\theta \rightarrow 0$, we obtain the following

differential equation:

$$\frac{dT}{d\theta} + \eta T = 0$$

The solution of this equation is:

$$T(\theta) = T_0 e^{-\eta\theta} \quad \text{where} \quad T(0) = T_0$$

Now $T(\theta)$ is a minimum at $\theta = \frac{\pi}{2}$

$$\text{or } T_{\text{MIN}} = T\left(\frac{\pi}{2}\right) = T_0 e^{-\frac{\eta\pi}{2}}; \quad \frac{T_{\text{MIN}}}{T_0} = e^{-\frac{\eta\pi}{2}}$$

At first unpolished aluminum was used as a curved support for the specimen and by measurements at room temperature it was found that $\eta = 0.38$. Thus $\frac{T_{\text{MIN}}}{T_0} = 0.55$ which was considered an excessive variation in uniformity. Since it is expected to be even higher at annealing temperatures, due to an increase in the coefficient of friction, a number of refractories were investigated. The most satisfactory material found was mica. This had an $\eta = 0.22$ or $\frac{T_{\text{MIN}}}{T_0} = 0.71$. It was found sufficient just to insert several thin sheets of mica between the aluminum and the specimen. The mica did not deteriorate to any noticeable extent during the heat treatment.

It is interesting to note that the minimum tension is determined only by the bending angle. Also the smaller the bending radius compared to the length of the straight sides, the larger will be the fraction of material at maximum tension.

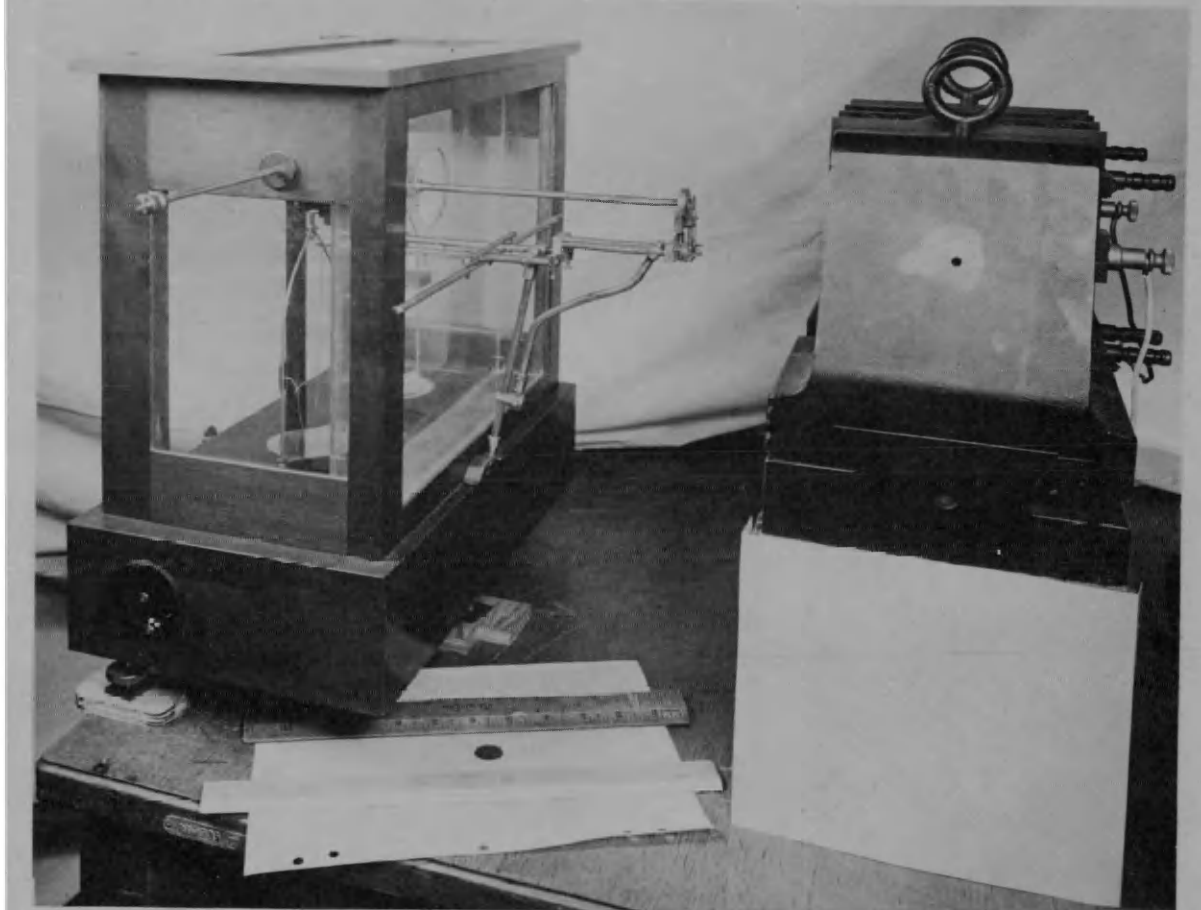
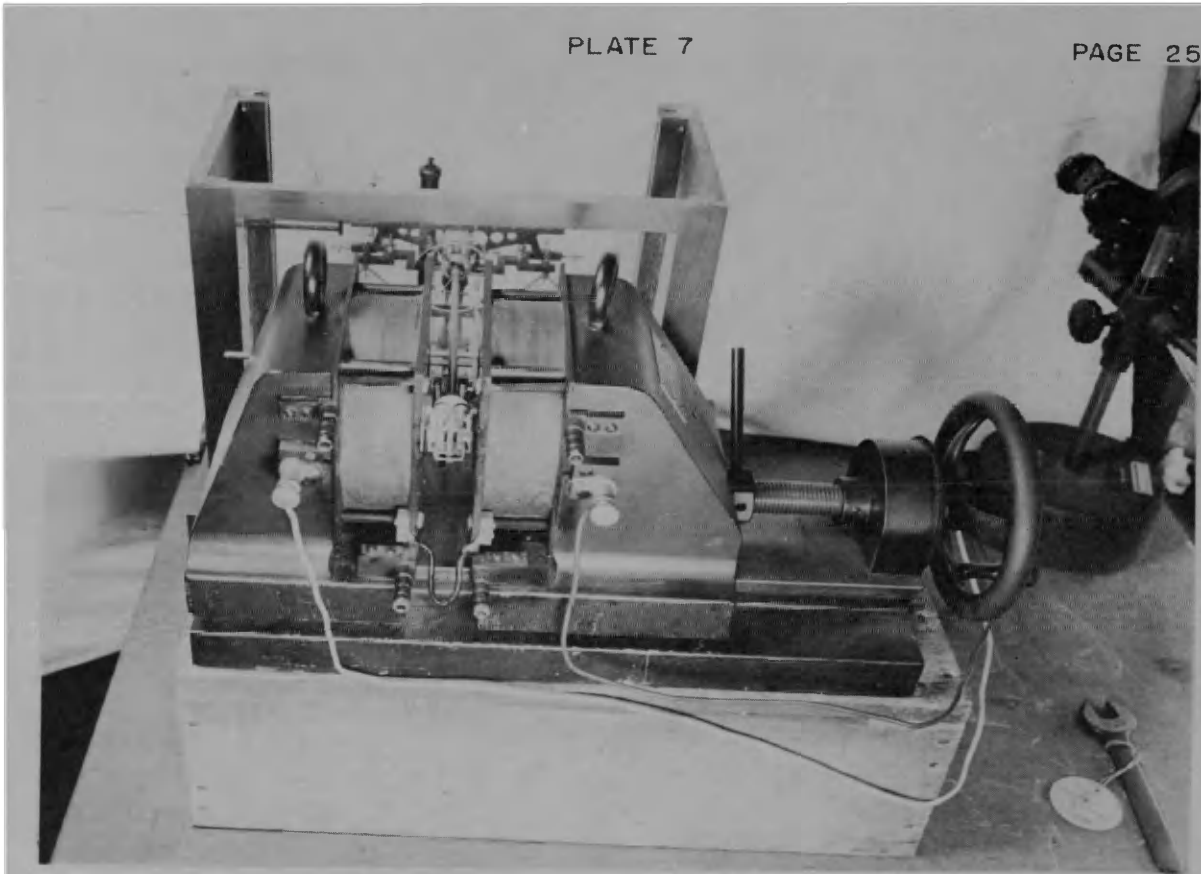
Now, the ring specimens were punched out of strips of the rolled alloy. Since the magnetic field used in permeability measurements was applied circumferentially, any tendency of preferred orientation of the grains would be averaged out in the measurement of ring specimens. The tension specimens were made out of strips cut parallel to the rolling direction. In the latter case, the magnetic measurements were made in the rolling direction. Consequently, grain orientation would influence the measurements. In order to minimize this, the rolling and heat treating procedure previously described was designed to suppress grain orientation.

The permeability measurements were made in a conventional manner using an L & N type HS 2285-e ballistic galvanometer employed as a fluxmeter. In such measurements it is necessary to wind primary and secondary windings on the specimen. Since the permeability of some of these nickel-iron alloys is very sensitive to mechanical stress, a method of properly supporting the test windings is essential. The ring specimens were inserted in an annular plastic box to support these windings. A plastic coil-form was erected about each tension specimen as shown in Plate 2 for the same

purpose. After the windings were put on the form, each specimen was inspected to insure that it could be moved freely in the box and therefore be free from external stress.

2. Anisotropy. The method used for measuring magnetic anisotropy was to measure the torque on a circular disc specimen when rotated in a uniform magnetic field parallel to the plane of the disc. The disc used was $3/4$ " in diameter and $.014$ " thick. The magnetic field was produced by an electromagnet. A field of 1500 oersteds was employed. This field was sufficiently large to substantially overcome the demagnetizing effects and saturate a disc of these dimensions.

Preliminary torque measurements were made on a disc suspended in the field at the end of a calibrated non-magnetic spiral spring. It was found that this spring was non-linear and calibration uncertain due to handling. Also different springs had to be used depending on the size of the anisotropy energy. Although some of these difficulties could be overcome by using a delicate suspension, it was decided to devise a wide range self-calibrating dynamometer. The instrument developed for this purpose is shown in Plate 7. The basic principal feature is the attachment of the disc at the end of a shaft coupled to a sensitive balance. The balance measures the torque on the disc in the field. The speed of measurement is augmented by use of a chain-o-matic balance. This dynamometer is self calibrating and has a



MAGNETIC DYNAMOMETER

very wide range. A gear arrangement permits orientating of the disc in a large number of discrete positions in the field.

The discs were processed with the other specimens and cooled at the prescribed cooling rate. The residual torque-curves (torque vs angle) were measured. The disc was then magnetic annealed and the torque curves were re-determined. The new curves were found to be approximately sine curves having a rotational period of 180° .

In most cases the residual torque had a rotational period of 180° with an equilibrium position ("easy" direction) at approximately 90° from the rolling direction. Since the cubic symmetry of the lattice would require a periodicity of 90° , magnetic anisotropy could not account for the residual torque. It is believed that the primary cause of residual torque was a slight lack of symmetry of the disc.

In the first tests magnetic annealing was performed with the applied field parallel to the rolling direction. This yielded a new "easy" direction nearly parallel to the rolling direction. The torque curves were plotted for each specimen before and after the magnetic annealing. These curves were subtracted graphically and a new curve was obtained. By integration the anisotropy energy introduced by magnetic annealing could be determined. The above method was inaccurate for small torques, and especially when the residual torques were not sinusoidal. Therefore, a new

procedure was devised. This procedure was to anneal the disc in a field parallel to its "easy" direction. Since in this case the "easy" direction was not changed by the magnetic anneal, it was sufficient to measure the areas under the torque curves of each specimen before and after the magnetic anneal and subtract. The average change in area under a half cycle was called the anisotropy energy introduced by magnetic annealing. The anisotropy energy density introduced by magnetic annealing, $\int \frac{f}{M_K}$, was obtained by dividing the above energy by the volume of the specimen. Both methods of determining the anisotropy energy density were employed on alloys pertinent to the argument to follow and close agreement was obtained.

SECTION III

RESULTS OF TENSION ANNEALING

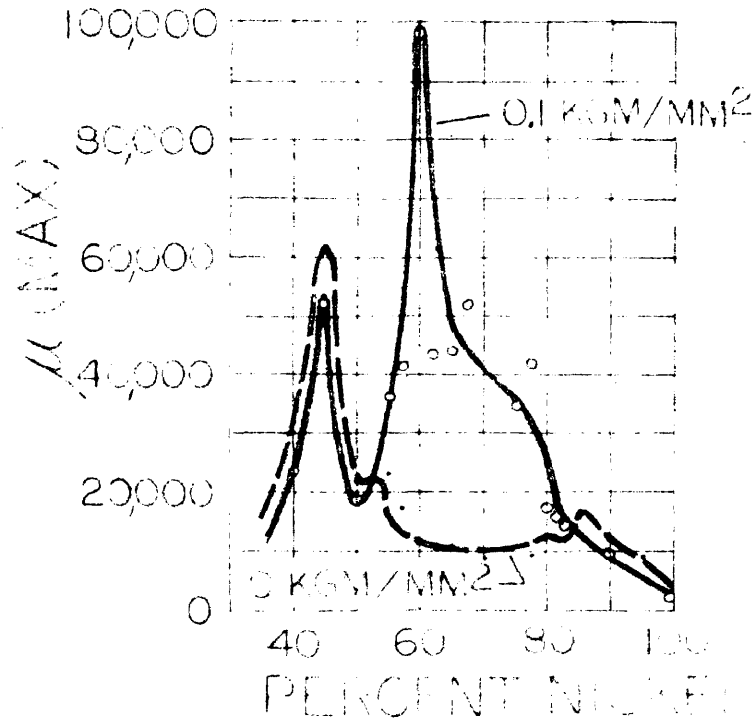
Preliminary experiments on a 72% nickel alloy with tension applied at various points in the annealing cycles, indicated that with sufficiently large tensions the magnetic properties were profoundly affected if the tension was applied during cooling, below Curie temperature. Experiments on annealing in a magnetic field have shown that the field influences the magnetic properties only when applied on cooling below the magnetic transformation temperature (2).

Another set of preliminary experiments were made using different rates of cooling during the tension anneal. It was found that the magnetic properties were influenced by the rate of cooling. Consequently, the cooling rate was standardized for all tension anneals.

Plate 8 shows the maximum permeability obtained by tension annealing for different compositions. Four different curves are drawn representing zero tension and three different values of tension applied during the anneal. In general, an increase in maximum permeability was accompanied by a decrease in coercive force, an increase in residual induction and initial permeability. A table of these magnetic properties for the 60% nickel alloy annealed under different values of tension is shown in Plate 8. In the discussion to follow only the maximum permeability will be considered since

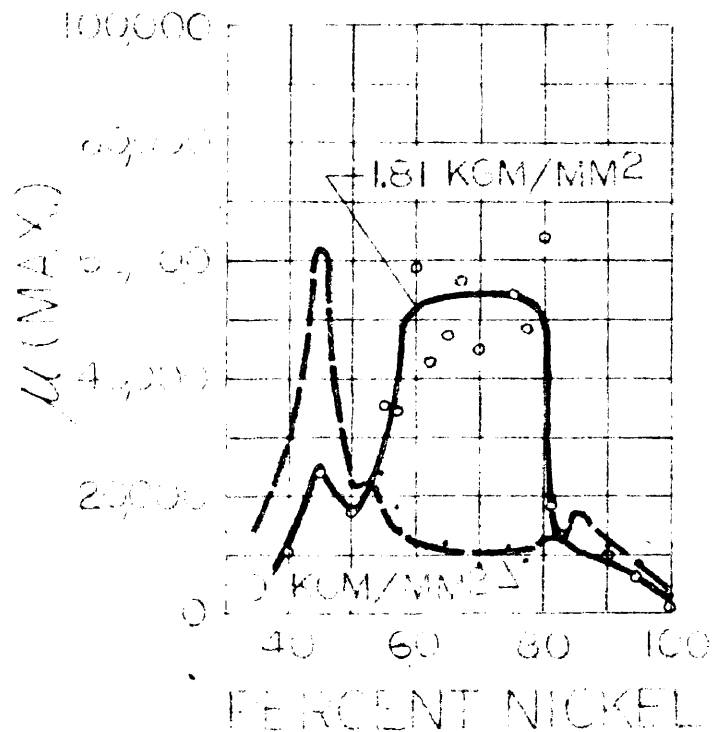
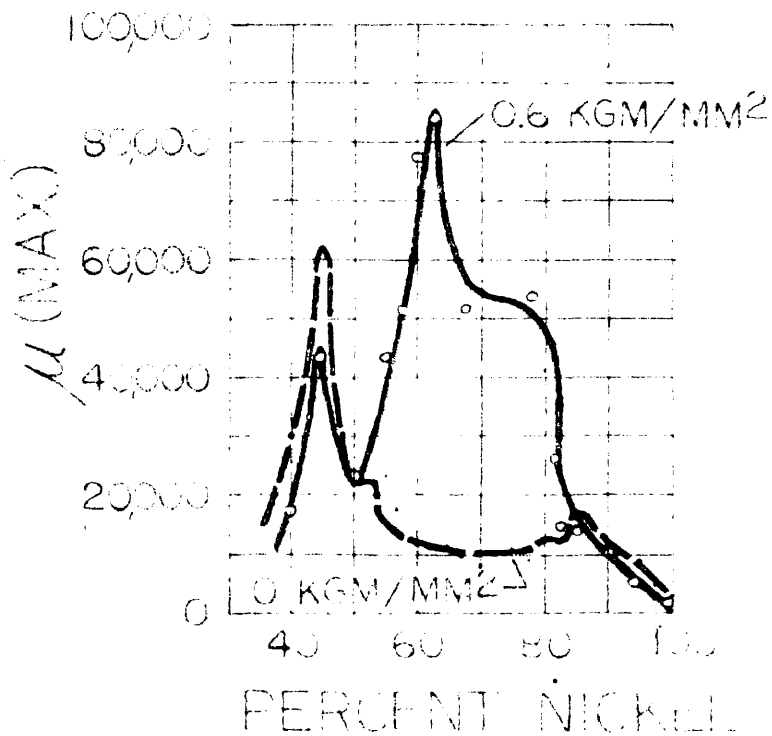
PLATE 8

MAXIMUM PERMEABILITY VS. COMPOSITION FOR TENSION ANNEALING



65% NICKEL

ANNEAL	μ_{20}	μ_{MAX}	$\frac{B_R}{B_M}$	H_c
0 KGM/MM ²	4200	11,126	.13	.1614
0.1 KGM/MM ²	14,438	98,634	.342	.0350
0.6 KGM/MM ²	14,438	78,180	.284	.0375
1.81 KGM/MM ²	12,760	59,470	.308	.0473

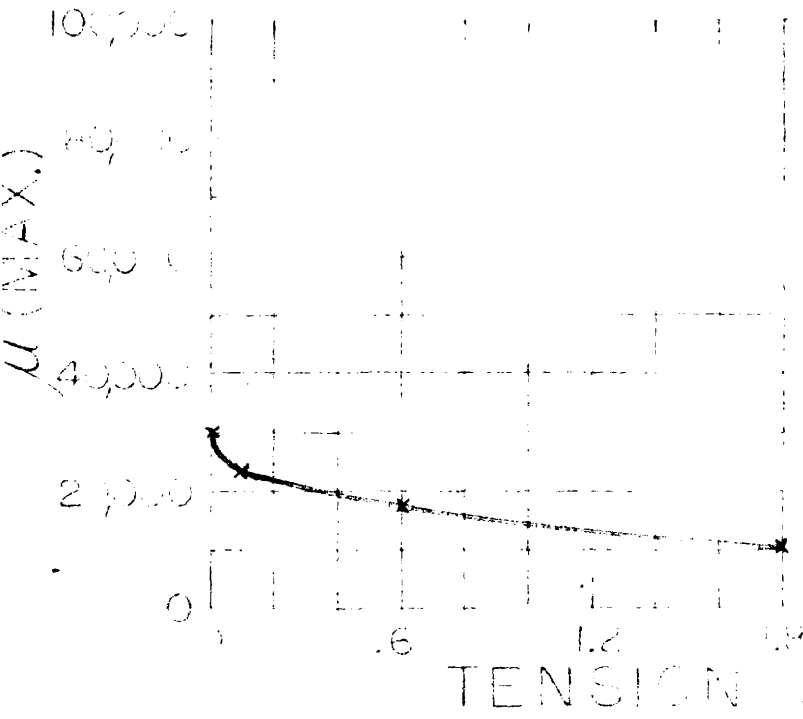


this was typical of the other magnetic characteristics. In general, a substantial increase in permeability is obtained on tension annealing for compositions between 50 and 82.5% nickel. Outside of this range the permeability is decreased by tension annealing. Plates 9-13 show the maximum permeability as a function of tension during annealing. It is seen that the greatest increase in permeability occurs at 60% nickel. The highest maximum permeability obtained is 99,000 for this alloy annealed under 0.1 kilograms per square millimeter of tension. This permeability is approximately 9 times as great as that obtained by ordinary annealing without tension.

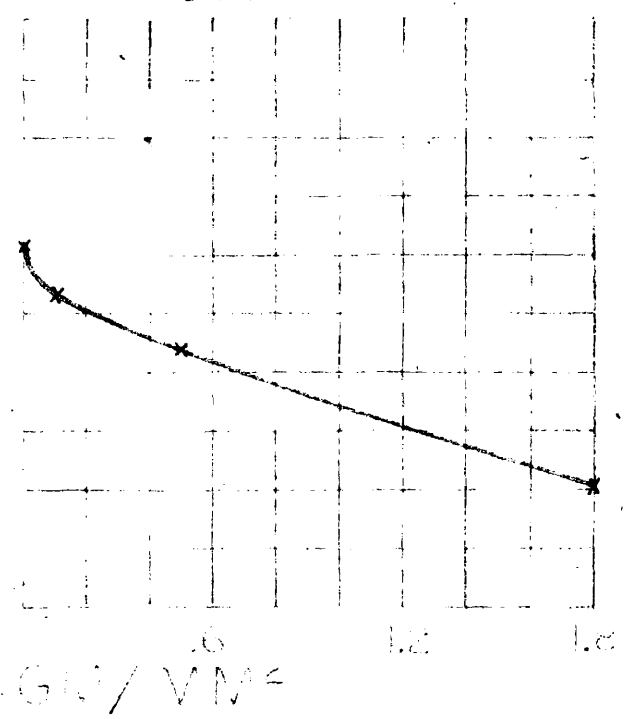
PLATE 9

MAXIMUM PERMEABILITY VS. TENSION
USED IN TENSION ANNEALING

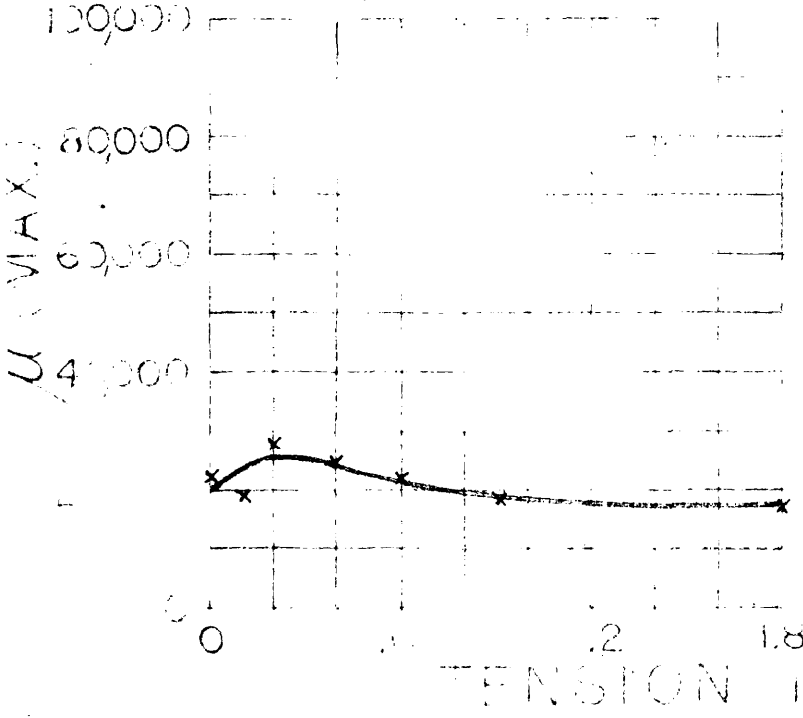
40% NICKEL



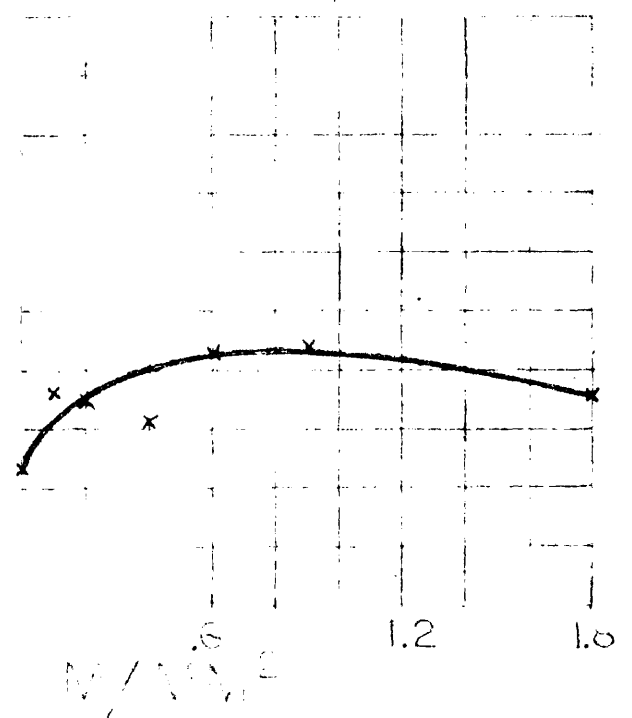
45% NICKEL



50% NICKEL

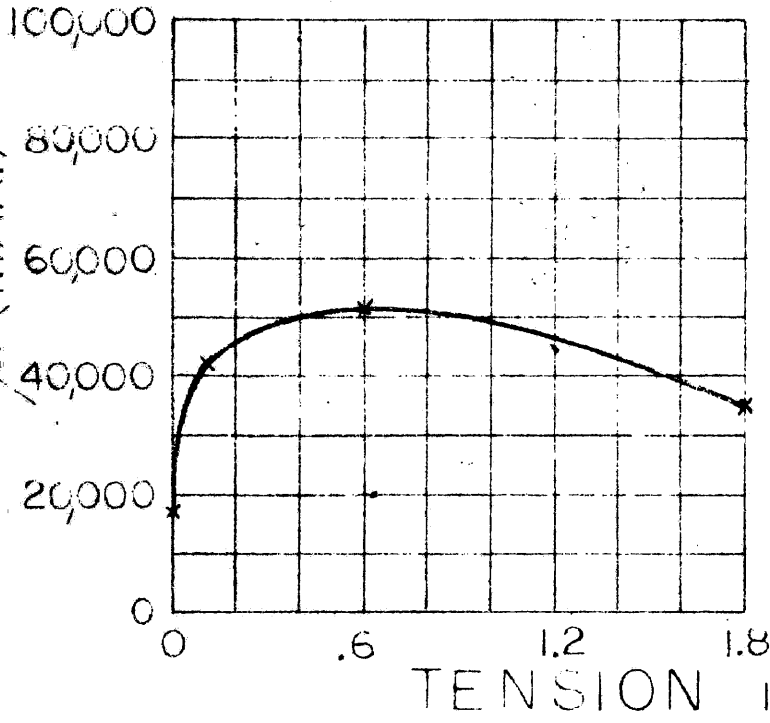


55% NICKEL

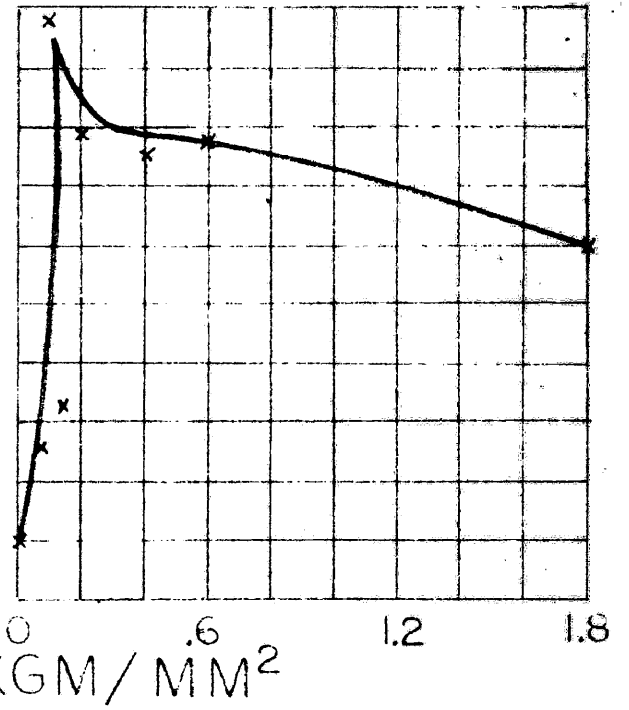


MAXIMUM PERMEABILITY VS. TENSION
USED IN TENSION ANNEALING

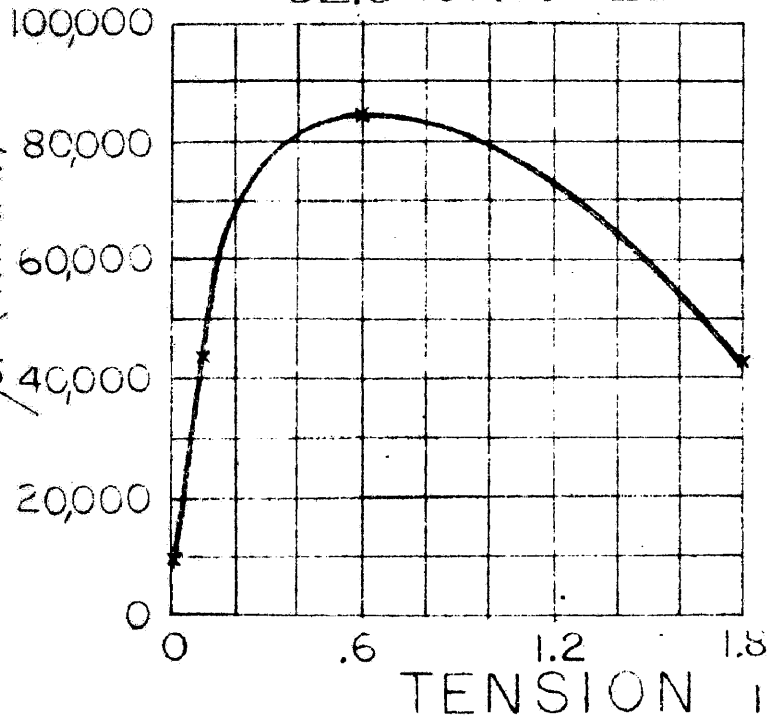
57.5 % NICKEL



60 % NICKEL



62.5 % NICKEL



65 % NICKEL

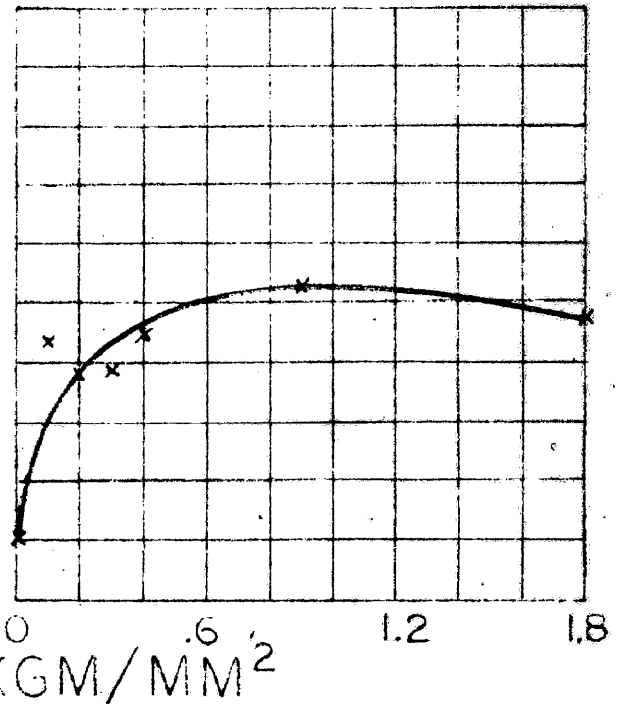
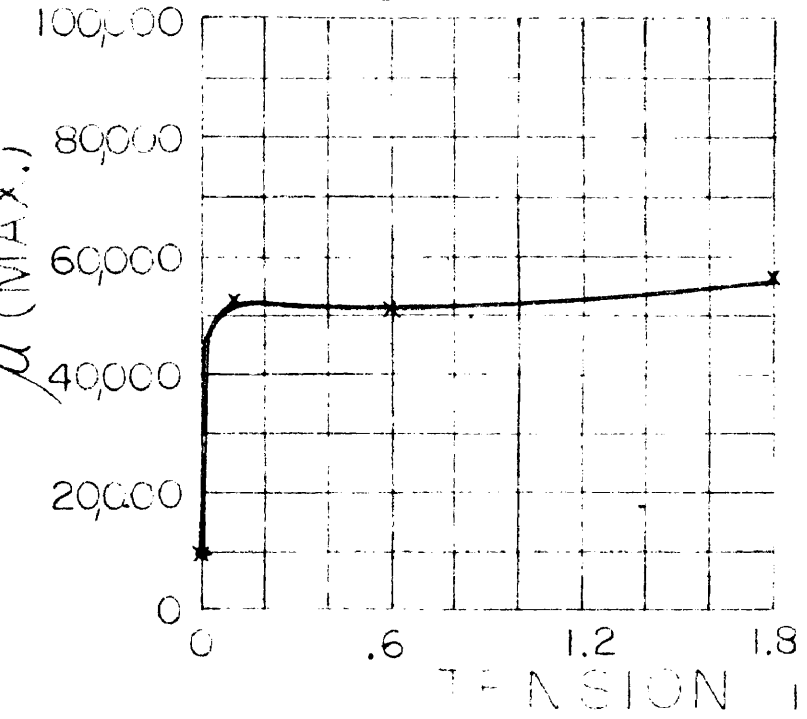


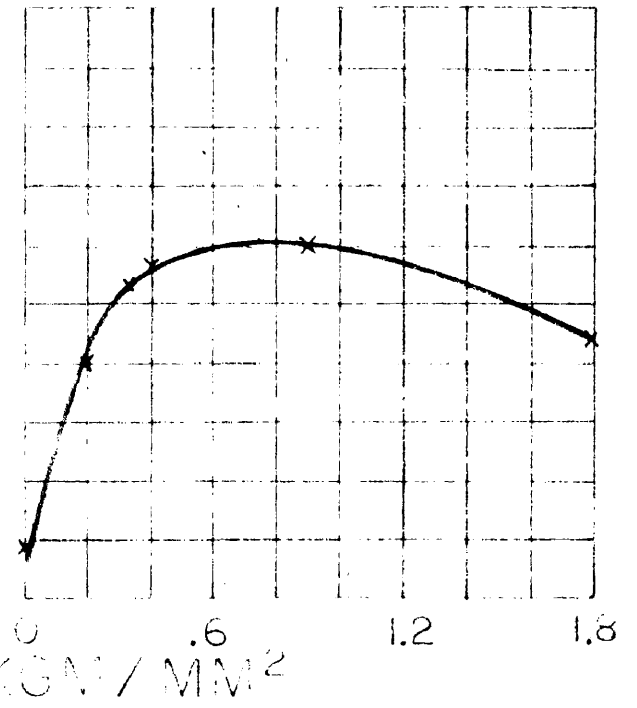
PLATE II

MAXIMUM PERMEABILITY VS. TENSION USED IN TENSION ANNEALING

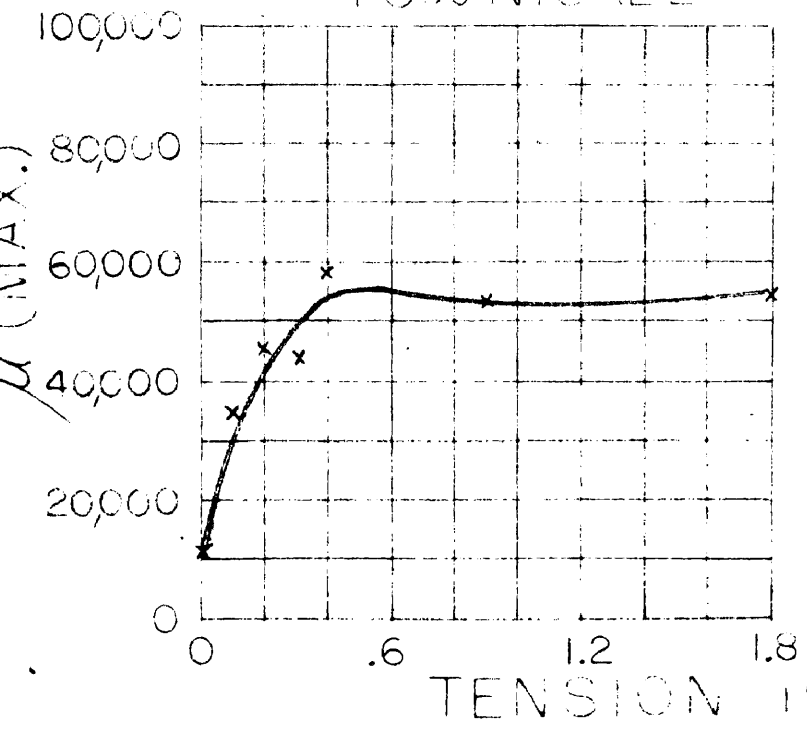
67.5% NICKEL



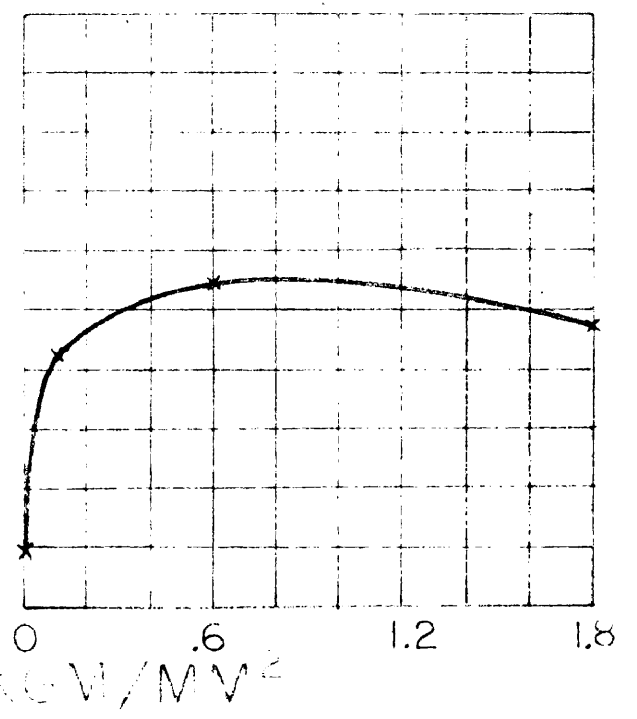
70% NICKEL



75% NICKEL

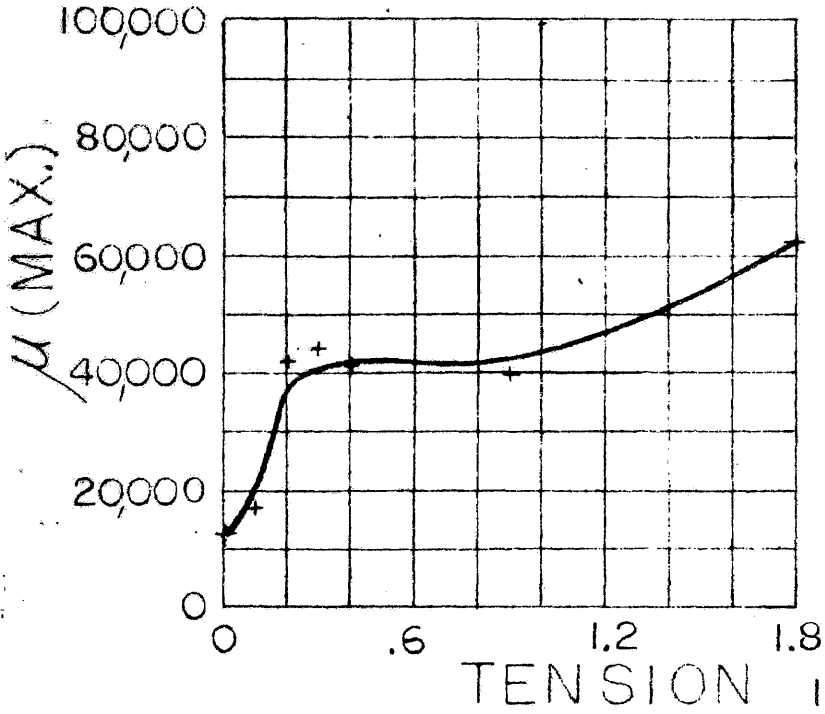


77.5% NICKEL

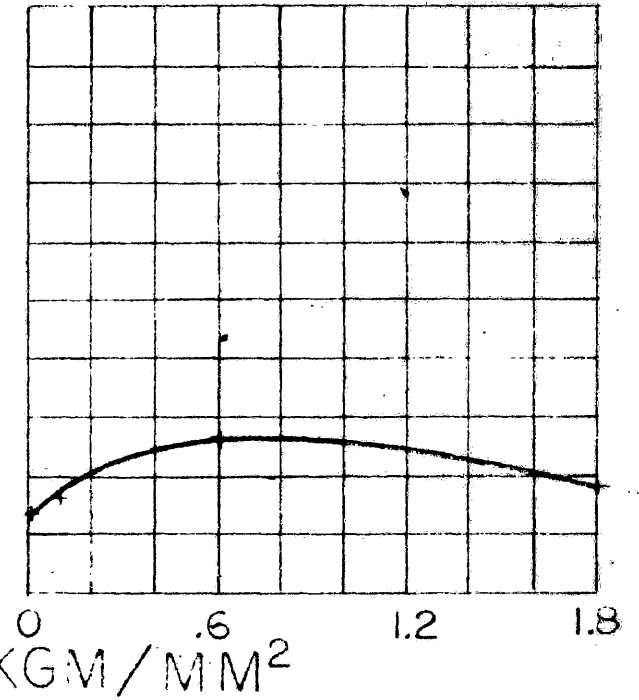


MAXIMUM PERMEABILITY VS. TENSION
USED IN TENSION ANNEALING

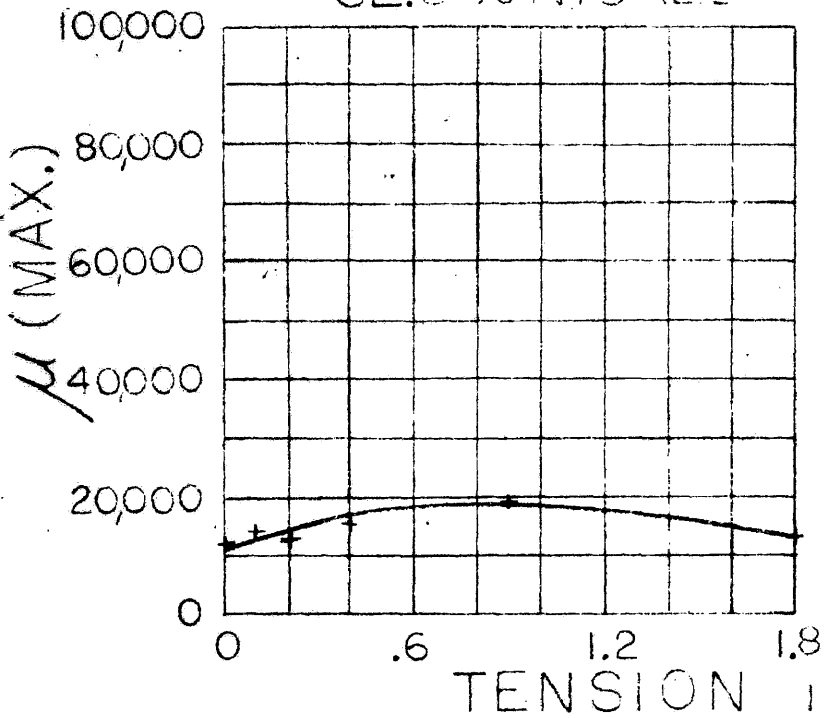
80% NICKEL



81% NICKEL



82.5% NICKEL



85% NICKEL

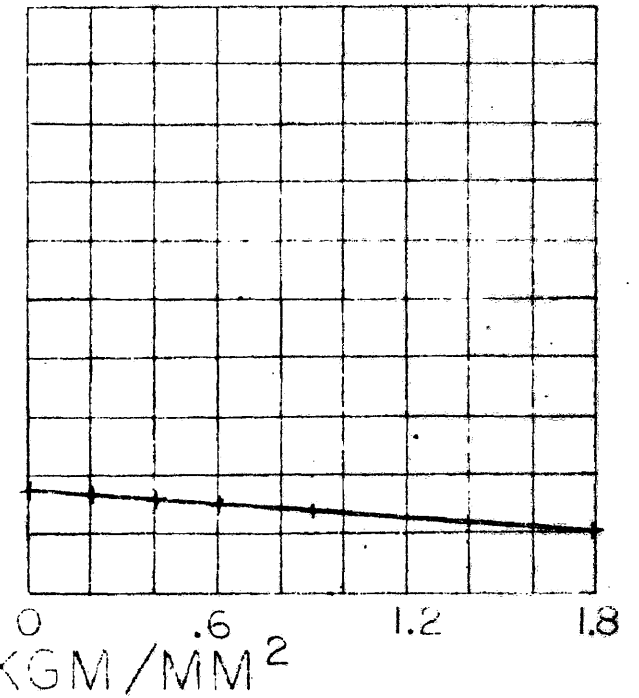
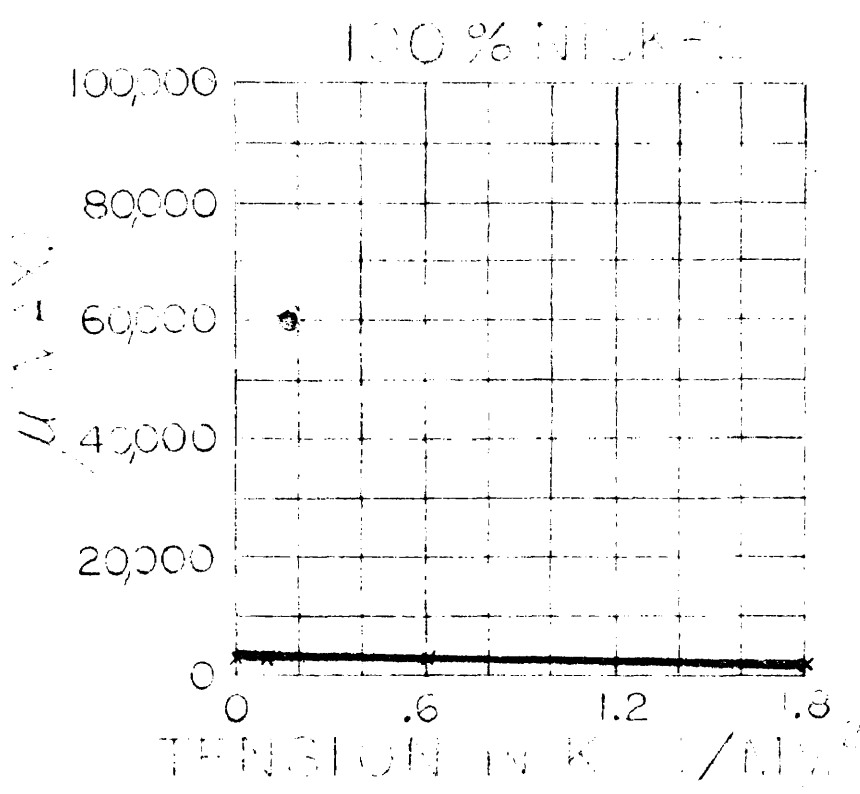
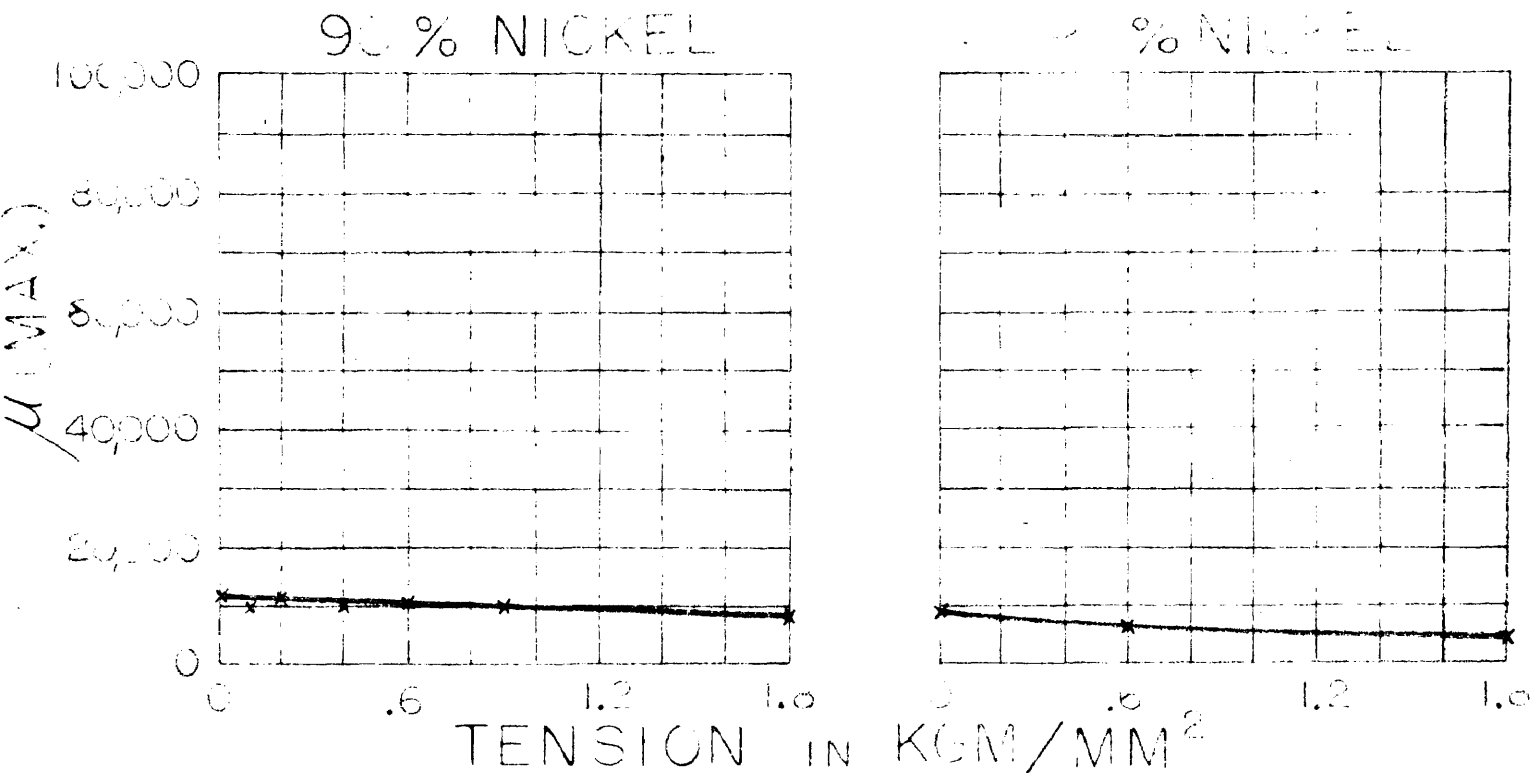


PLATE 13

MAXIMUM PERMEABILITY VS. TENSION USED IN TENSION ANNEALING



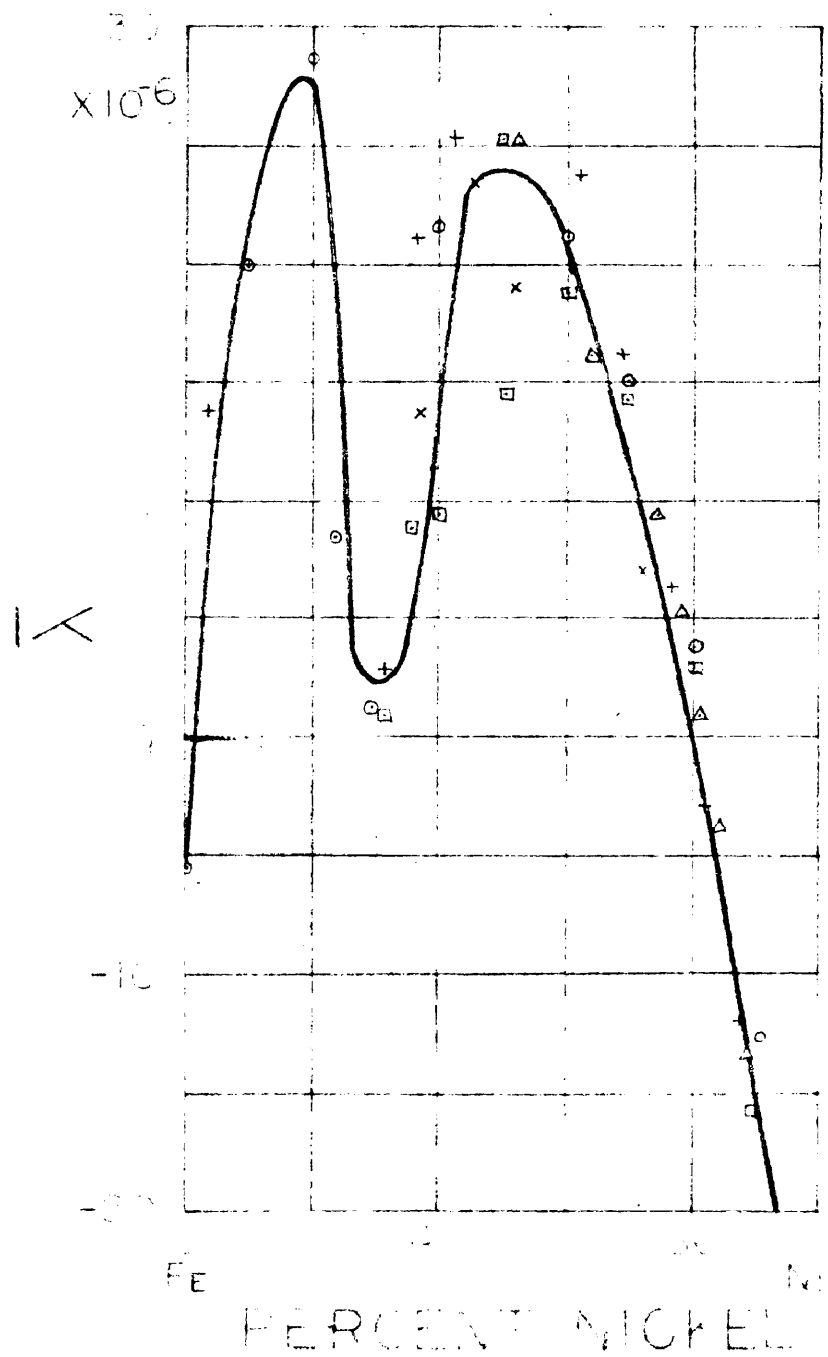
SECTION IV

INTERPRETATION OF RESULTS

The magnetic characteristics of nickel-iron alloys under the influence of mechanical stress at ambient temperatures has been investigated by others. They found that the maximum permeability increased with tension in the alloys for which the saturation polycrystalline magnetostriction constant, $\bar{\lambda}$, was positive. Conversely, they found that the maximum permeability decreased when $\bar{\lambda}$ was negative. It might be expected that the results of tension annealing would be similar to results obtained on materials under stress at ambient temperature. Since we are primarily interested in explaining effects observed at different compositions, the saturation polycrystalline magnetostriction constant is shown in Plate II as a function of nickel content. It is seen that the decrease in permeability on tension annealing for compositions greater than 82.5 nickel may be explained by the fact that $\bar{\lambda}$ is negative for these compositions. One of the outstanding results of this investigation was the decrease in permeability on tension annealing for compositions having less than 50% nickel. This cannot be explained on the prior theory since $\bar{\lambda}$ is positive for these compositions.

PLATE 14
SATURATION MAGNETOSTRICTION
POLYCRYSTALLINE Ni-Fe ALLOYS
ACCORDING TO DIFFERENT AUTHORS

FROM BECKER AND DÖRING, FERROMAGNETISMUS
P. 261

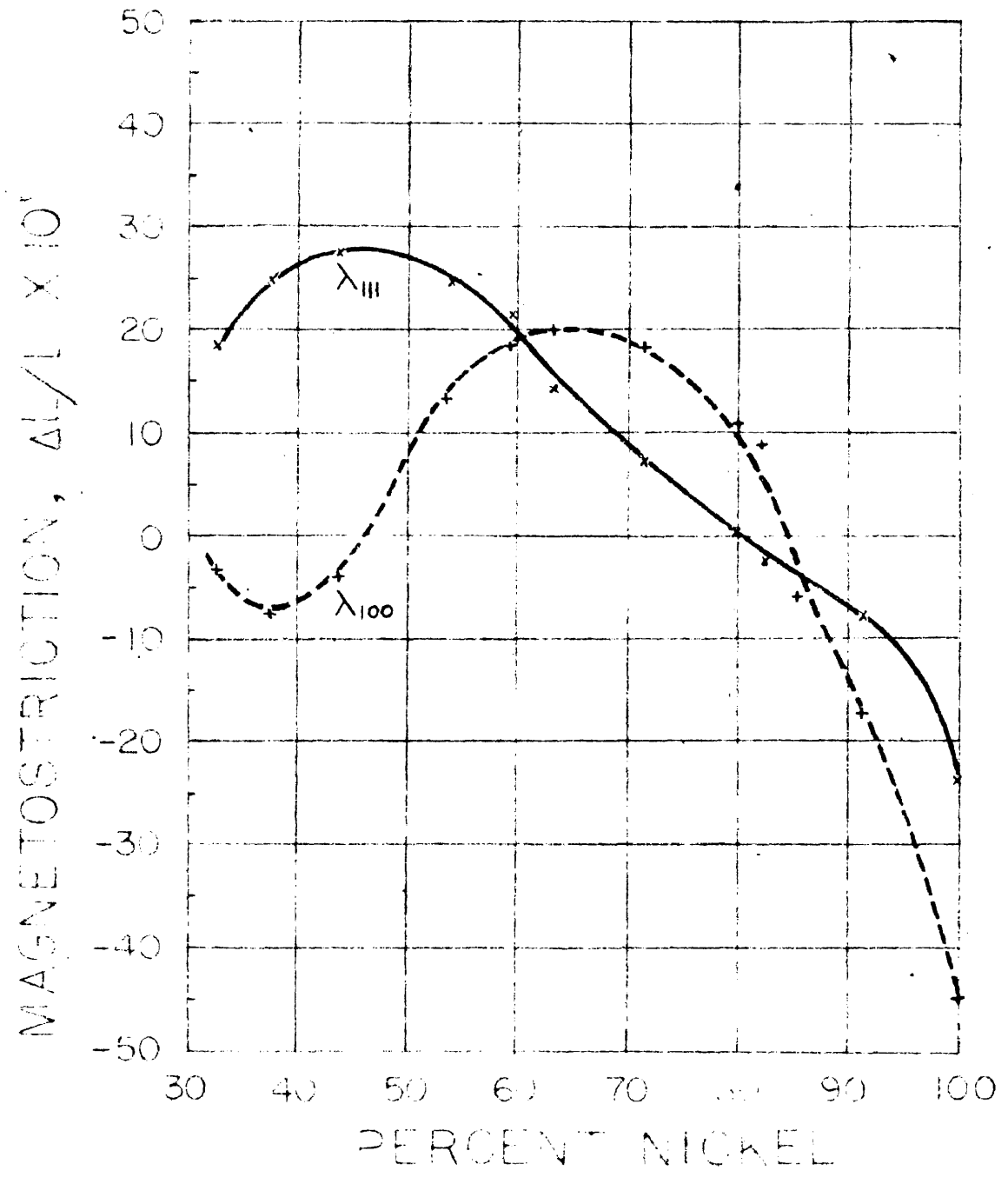


It has been found that in general magnetostriction is not isotropic but depends on orientation with respect to the crystal axis. Plate 15 is a reproduction of Lichtenberger's data on the saturation magnetostriction constants for two principal crystallographic directions $[100]$ and $[111]$. The constants are designated as λ_{100} and λ_{111} , respectively. It is seen that λ_{100} becomes negative in the range of composition under consideration. Since each of the polycrystalline materials under investigation is really an aggregate of single crystals, $\bar{\lambda}$ may be considered as an average of λ_{100} and λ_{111} properly weighted according to the distribution of the orientation of individual grains. It is evident that λ_{100} negative is not incompatible with $\bar{\lambda}$ positive in the 40-50% nickel range since λ_{111} is positive. It should be mentioned that the data shown in Plate 15 has been shown to be in error since the volume magnetostriction was not eliminated in the measurements (3). The volume magnetostriction is greatest near 30% nickel and the data at the lower nickel range is in greatest error.

In order to understand the role of λ_{100} , in tension annealing, a discussion of magnetic anisotropy is in order. In fact anisotropy considerations are important even when only isotropic magnetostriction is considered, since the tensile forces tending to orientate the magnetization vector must compete against the crystalline forces, the latter being a manifestation of magnetic anisotropy energy. The anisotropy energy density, f_K , may be formally written as a power

PLATE 15
SATURATION MAGNETOSTRICTION
SINGLE CRYSTAL Ni-Fe ALLOYS
FOR TWO PRINCIPAL CRYSTALLOGRAPHIC
DIRECTIONS

FROM REICHTENSBERGER, ANN. PHYS., 1874, 1, 310-10



series of $\alpha_1, \alpha_2, \alpha_3$, the direction cosines of the magnetization vector with respect to the crystal axis. It is known from experiments that the resulting expression must have cubic symmetry of the crystal lattice. Furthermore, the magnetization itself has certain symmetry requirements. Thus it can be shown (4) that to the first approximation

$$f_k = K_1 (\alpha_1^2 \alpha_2^2 + \alpha_2^2 \alpha_3^2 + \alpha_1^2 \alpha_3^2)$$

In this expression K_1 is the cubic anisotropy constant and it is given as a function of composition in Plate 16.

To obtain the equilibrium orientation of the magnetization vector, or the so called "easy" direction of magnetization, we must find the direction that makes f_k a minimum, or $\delta f_k = 0$. By differentiation

$$\delta f_k = \frac{\partial f_k}{\partial \alpha_1} \delta \alpha_1 + \frac{\partial f_k}{\partial \alpha_2} \delta \alpha_2 + \frac{\partial f_k}{\partial \alpha_3} \delta \alpha_3$$

The α 's are connected by the following equation of constraint:

$$\alpha_1^2 + \alpha_2^2 + \alpha_3^2 = 1$$

and by differentiation

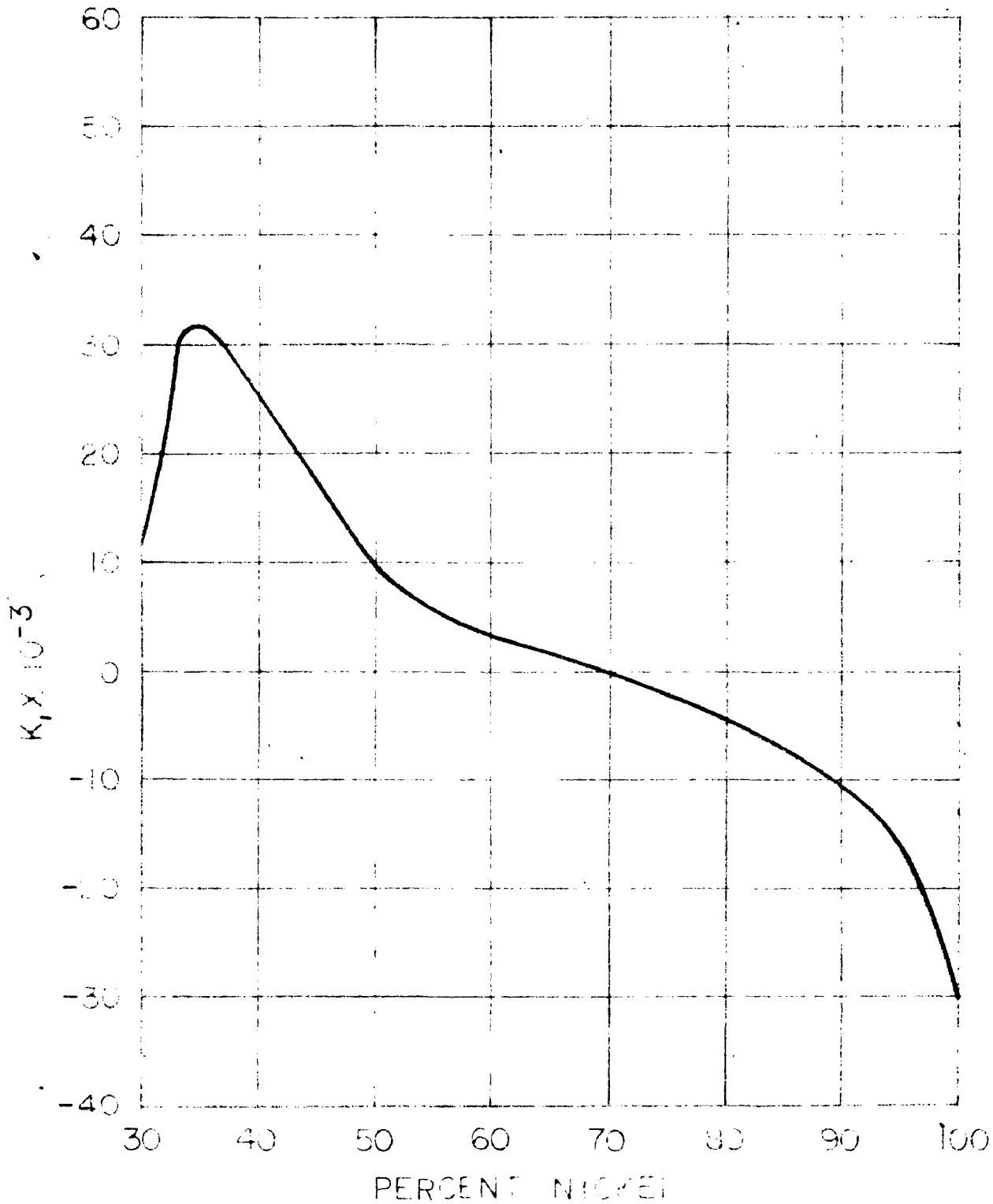
$$\alpha_1 \delta \alpha_1 + \alpha_2 \delta \alpha_2 + \alpha_3 \delta \alpha_3 = 0$$

By addition and use of LaGrange's undetermined multiplier, λ ,

$$\left(\frac{\partial f_k}{\partial \alpha_1} + \lambda \alpha_1 \right) \delta \alpha_1 + \left(\frac{\partial f_k}{\partial \alpha_2} + \lambda \alpha_2 \right) \delta \alpha_2 + \left(\frac{\partial f_k}{\partial \alpha_3} + \lambda \alpha_3 \right) \delta \alpha_3 = 0$$

Since we have two independent variables, e.g. α_2, α_3 and a

PLATE 16
CUBIC ANISOTROPY CONSTANT, K_1
FOR NI-Fe ALLOYS



FROM UNPUBLISHED DATA OF H. N. WILLIAMS

constant λ to be determined, we may set

$$\frac{\partial f_k}{\partial \alpha_1} = -\lambda \alpha_1 = 2 K_1 \alpha_1 (1 - \alpha_1^2)$$

$$\frac{\partial f_k}{\partial \alpha_2} = -\lambda \alpha_2 = 2 K_1 \alpha_2 (1 - \alpha_2^2)$$

$$\frac{\partial f_k}{\partial \alpha_3} = -\lambda \alpha_3 = 2 K_1 \alpha_3 (1 - \alpha_3^2)$$

Solutions to this set of minimal equations are $\alpha_1^2 = \alpha_2^2 = \alpha_3^2 = \frac{1}{3}$ or $[111]$ and $\alpha_1 = 1, \alpha_2 = \alpha_3 = 0$ or $[100]$ and equivalent crystallographic directions. By substitution in the equations for f_k we find that if $K_1 > 0$, $[100]$ is an "easy" direction of magnetization and if $K_1 < 0$, $[111]$ is an "easy" direction. Thus we see that a decrease in λ_{100} with composition might seriously affect our polycrystalline results since $[100]$ is an easy direction of magnetization in the range of compositions under consideration.

In order to understand results obtained by annealing, one should consider how the magnetostriction and anisotropy behave at elevated temperatures. Now it is known (5) that in general the anisotropy energy falls off quite rapidly with increasing temperature. The magnetostriction also decreases with temperature, at least for the only case known to the author on which experimental data is available (6). However, the anisotropy diminishes at a faster rate than the magnetostriction. When the anisotropy is small at room temperature we can neglect it in explaining effects taking place at elevated temperatures. When it is fairly large at room temperatures it will still be a second order effect at

elevated temperatures, particularly when the magnetostriction is large. In the latter case we will include it whenever convenient for analysis. Let us now consider the cases in which the magnetostriction is anisotropic (Case I) and isotropic (Case II).

1. Case I. Anisotropic Magnetostriction. Let us consider only the favorably orientated grains, the crystal axis of which is parallel to the applied tension. When there are only two magnetostriction constants λ_{100} and λ_{111} and a uniform tensile stress, T , acting with direction cosines, $\gamma_1, \gamma_2, \gamma_3$, with respect to the crystal axis, the magnetostriction part of the energy density, f_{me} , is (1)

$$f_{me} = -\frac{3}{2} \lambda_{100} (\alpha_1^2 P_{11} + \alpha_2^2 P_{22} + \alpha_3^2 P_{33}) \\ - 3 \lambda_{111} (\alpha_1 \alpha_2 P_{12} + \alpha_2 \alpha_3 P_{23} + \alpha_3 \alpha_1 P_{31})$$

where $P_{ik} = T \gamma_i \gamma_k$ are the stress components.

$$\text{In Case I, } f_{me} = -\frac{3}{2} \lambda_{100} \alpha_1^2 T$$

$$\text{and } \frac{\partial f_{me}}{\partial \alpha_1} = -3 \lambda_{100} \alpha_1 T$$

The minimal equations previously considered now become

$$-\lambda \alpha_1 = \alpha_1 [2 K_1 (1 - \alpha_1^2) - 3 \lambda_{100} T] \\ -\lambda \alpha_2 = 2 K_1 \alpha_2 (1 - \alpha_2^2) \\ -\lambda \alpha_3 = 2 K_1 \alpha_3 (1 - \alpha_3^2)$$

Of course if $\lambda_{100} = 0$ there will be no effect of tension in this case. This roughly corresponds to alloys containing about 50% nickel.

If $K_1 > 0$ which is true for 40-60% Ni, solutions yielding a minimum are:

$$\text{When } \lambda_{100} > 0 \quad \alpha_1 = 1, \quad \alpha_2 = \alpha_3 = 0 \quad \text{or } [100]$$

$$\text{When } \lambda_{100} < 0 \quad \alpha_1 = 0, \quad \alpha_2 = 1, \quad \alpha_3 = 0 \quad \text{or } [010]$$

$$\alpha_1 = 0, \quad \alpha_2 = 0, \quad \alpha_3 = 1 \quad \text{or } [001]$$

Thus if $\lambda_{100} > 0$, tension annealing will tend to orientate the domains of the favorably orientated grains along the tension direction. When $-\lambda_{100} > 0$, tension will create a preference for domains orientated at right angles to the tension direction.

2. Case II. Isotropic Magnetostriction. In this case we consider isotropic magnetostriction or $\lambda_{100} = \lambda_{111} = \bar{\lambda}$

Now f_{me} becomes

$$f_{me} = -\frac{3}{2} \bar{\lambda} T [\alpha_1^2 \gamma_1^2 + \alpha_2^2 \gamma_2^2 + \alpha_3^2 \gamma_3^2 + 2(\alpha_1 \alpha_2 \gamma_1 \gamma_2 + \alpha_2 \alpha_3 \gamma_2 \gamma_3 + \alpha_1 \alpha_3 \gamma_1 \gamma_3)]$$

Now the angle ψ between T and the magnetization vector is determined by

$$\cos \psi = \alpha_1 \gamma_1 + \alpha_2 \gamma_2 + \alpha_3 \gamma_3$$

and

$$\cos^2 \psi = \alpha_1^2 \gamma_1^2 + \alpha_2^2 \gamma_2^2 + \alpha_3^2 \gamma_3^2 + 2(\alpha_1 \alpha_2 \gamma_1 \gamma_2 + \alpha_2 \alpha_3 \gamma_2 \gamma_3 + \alpha_1 \alpha_3 \gamma_1 \gamma_3)$$

$$\text{Thus } f_{me} = \frac{3}{2} \bar{\lambda} T \cos^2 \psi$$

We assume that we can neglect K_1 for this case at elevated temperatures which is reasonable for most of the alloys between 50 and 95% Ni. The minimal conditions are:

$$\text{When } \bar{\lambda} > 0 \quad \psi = 0, \pi$$

$$\text{When } \bar{\lambda} < 0 \quad \psi = \frac{\pi}{2}, \frac{3\pi}{2}$$

Thus we see that with positive isotropic magnetostriction, tension tends to line the magnetic domains along the tension direction independent of the orientation of the individual grains. On the other hand, with negative isotropic magnetostriction, tension orients the magnetic domains at right angles to the tensile force. If the anisotropy energy is large, the effect of crystal forces would have to be taken into account. They can be neglected for nickel contents between 50 and 90%, since the anisotropy is small at ambient temperatures and negligible at annealing temperatures.

3. Magnetization Process. According to the domain theory, in the demagnetized state, magnetic materials are composed of a large number of microscopic regions or domains, each magnetized to saturation, but so orientated that there is no net macroscopic magnetization. Each domain is orientated along an "easy" crystallographic direction in absence of any disturbing influences such as strains. When a small field is applied in a given direction, favorably orientated domains grow reversibly at the expense of unfavorably orientated domains. In larger fields irreversible 90° and 180° rotations also take place. In fields approaching saturating fields, a reversible rotation takes place in which the domains are rotated away from their "easy" direction and into the field direction.

According to domain theory (7), 180° rotations can occur at a lower energy than 90° rotations. Thus a higher permeability can be obtained if the proportion of 180°

rotations to 90° rotations can be increased. In Case I we have shown that in favorably orientated grains, and positive λ_{100} and $K_1 > 0$, tension annealing will produce a preference for orientation of the magnetization along that particular "easy" axis parallel to the tension direction rather than other normally equally preferred "easy" directions. In Case II with a positive $\bar{\lambda}$ and negligible anisotropy, tension will create an "easy" direction in the tension direction irrespective of the orientation of each particular grain. Both of the above situations imply a preference of 180° rotations. In both cases negative magnetostriction leads to a preference normal to the tension direction. This implies that 90° rotations will be preferred. Thus we see how tension annealing will affect the relative proportions of 180° and 90° reversals and consequently the maximum permeability.

It follows that the greatest increase in permeability can be obtained by tension annealing if the anisotropy is low and the magnetostriction is isotropic and positive. In addition, for small tensions, $\bar{\lambda}$ should be large. These conditions are satisfied in the 60% nickel alloy and explains the results obtained.

While the character of observed changes in permeability produced by tension annealing has been explained, no explanation has been given of the more fundamental problem on the mechanism of retention. In other words, why does the alloy retain the influence of tension applied during

annealing after the alloy has been cooled down to ambient temperature and the tension removed? An answer to this fundamental question cannot be presented at this time. The mechanism of retention is probably a special case of a more general problem including the so-called "Permalloy Problem" and the mechanism of magnetic annealing. Neither of these problems have ever been completely solved. We have repeated some experiments on the alloys made for this investigation, to verify results obtained by others and to eliminate any experimental discrepancies between our problem and the other two problems. We will present some new results which have been obtained and which may ultimately lead to a solution of the more general problem. The remainder of this dissertation will be confined to the other two problems.

SECTION V

THE PERMALLOY PROBLEM

Classically, the best heat treatment for soft magnetic material was to cool down slowly from elevated temperatures. It was believed that this prevented the mechanical strains that would be introduced by rapid cooling. A number of investigators examined the nickel-iron series and taking the precautions used for annealing iron they concluded that the various nickel-iron alloys were not as good magnetically as iron.

G. W. Elmen (8) discovered that very remarkable magnetic permeabilities could be obtained by rapidly cooling certain nickel-iron alloys from their magnetic transformation temperature to ambient temperature. He obtained the highest permeability at 78.5% nickel. The nickel-iron alloys containing more than 30% nickel were called permalloys.

In order to explain the effect of rapid cooling, Elmen postulated that quenching retained a solid solution of the two constituents. On slow cooling or baking, a segregation took place. The solid solution was softer magnetically than the segregated material. He supported this explanation by resistivity data. The quenched material had a higher resistivity than the baked material which would be expected if segregation took place. In addition he noted that the

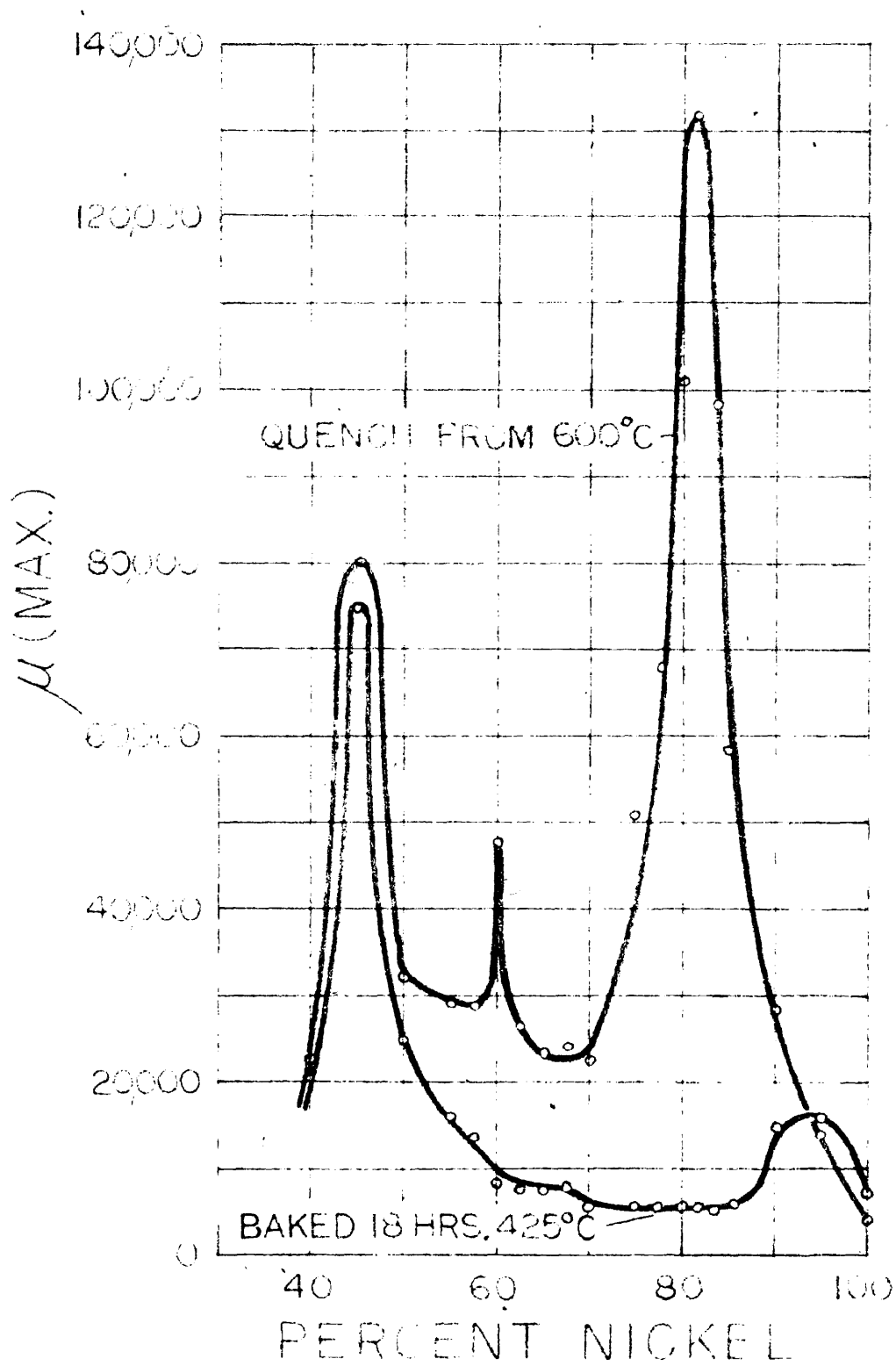
highest initial permeability occurred close to that composition where the magnetostriction was zero.

The discovery of this permalloy effect initiated intensive investigations in this field. It has now been established (9) that a superstructure exists at a composition corresponding to Ni_3Fe or 76% nickel. The reason why superstructure should be harder magnetically than solid solution has not been explained.

The effect on rapid cooling in hydrogen of the nickel-iron alloys used in this investigation is shown in Plate 17. We have obtained the highest maximum and initial permeabilities at 81% nickel, although only the maximum permeability has been shown. The permeabilities obtained are higher than that reported by Elmen, due to improvements in melting and heat treating techniques. The reason why we obtained the highest permeability at 81% nickel instead of 78.5% nickel found by Elmen, is attributed to a slower rate of cooling used in our investigation.¹ The lower curve in Plate 17 shows the effect of baking for 18-hours at 425°C . It is seen that the maximum permeability is almost independent of composition between 60 and 90% nickel and lower than that which can be obtained for iron. The high permeability obtained on baking 45% nickel is probably due to advanced

¹Elmen rapidly cooled in air by placing the magnetic specimen on a copper plate, whereas we have merely quenched in hydrogen by withdrawing the specimen to the cold part of the annealing box.

PLATE 17

EFFECT OF COOLING RATE
ON Ni-Fe ALLOYS

hydrogen heat treating techniques that were not available when the nickel-iron series was first investigated. The increase in permeability on quenching at 60% nickel has never appeared in the literature before. This could be due to advances we have made in purification techniques of melting and hydrogen annealing.

Becker and Kersten (10) have developed a theoretic formula for the highest initial permeability which can be obtained in absence of a large preponderance of 180° reversals. The equation is:

$$(\mu_0)_{\text{MAX}} = \left(-\frac{8\pi}{9} \frac{I_s^2}{\bar{\lambda}^2} E \right)$$

where I_s is the intensity of magnetization at saturation and E is the modulus of elasticity. According to their theory internal strains resist the movement of magnetic domains. But due to magnetostriction, there will be an inherent lattice strain introduced when the material cools down below the magnetic transformation temperature. At ambient temperature, the smallest possible strain will be $\bar{\lambda}$. Thus, when $\bar{\lambda}$ is zero, the initial permeability will be infinitely large.

One difficulty in Becker and Kersten's theory is that the highest permeability was obtained at 78.5% nickel but the magnetostriction was reported as zero at 81% nickel. Since we have obtained our highest maximum permeability at 81%, it was decided to actually measure where the magnetostriction was zero for the same alloys on which the per-

meabilities were measured. By using strain gauge techniques and interpolating, it was found that the saturation polycrystalline magnetostriction was zero at 83.5% nickel. Therefore, the discrepancy in the above formula has not been resolved.

Some investigators have explained the above discrepancy by stating that 78.5% nickel is a favorable composition where the anisotropy and magnetostriction are both small. Since it is desirable to have these two factors a minimum, 78.5% happens to be the optimum composition.

SECTION VI

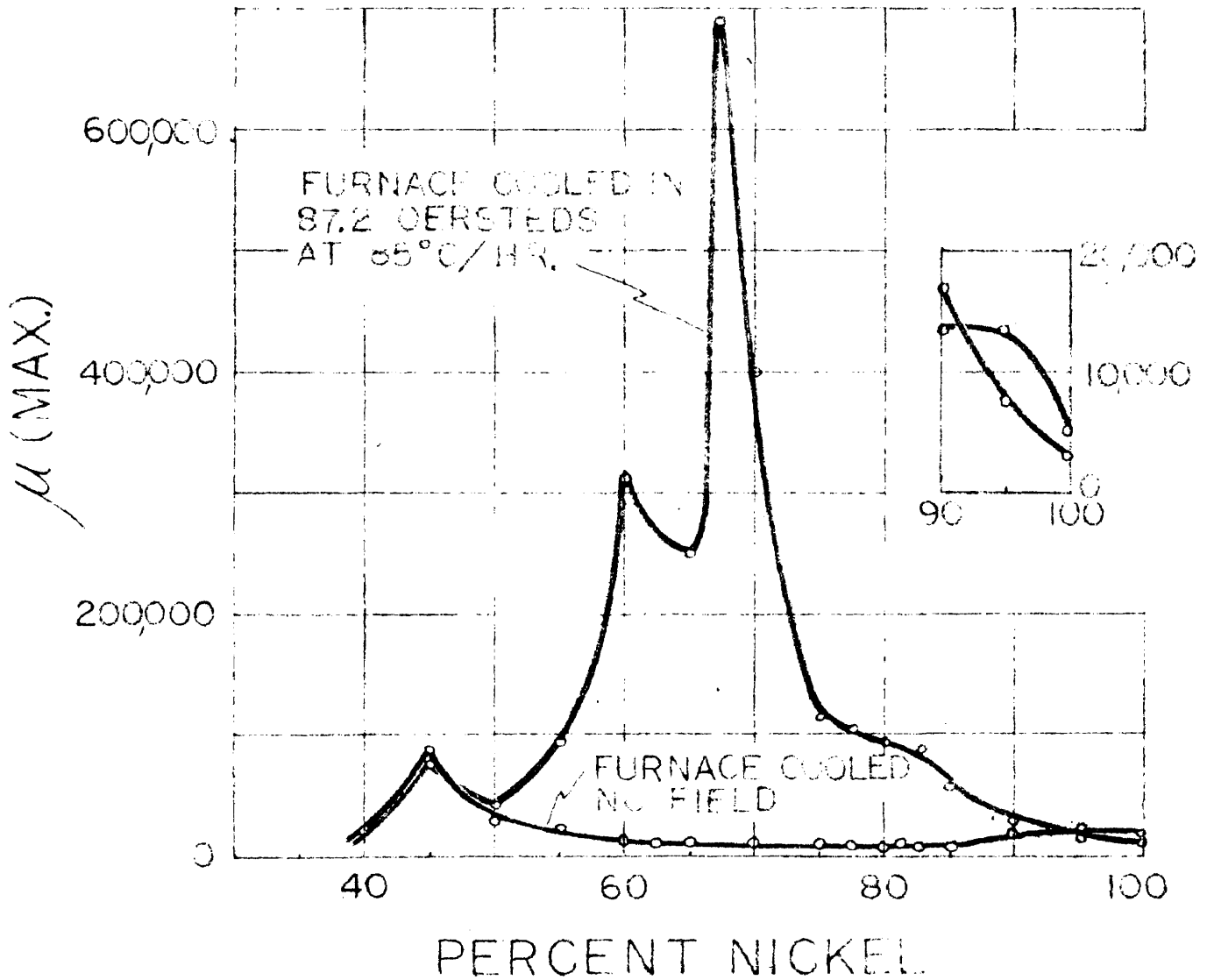
MAGNETIC ANNEALING

Experiments on cooling magnetic materials in a magnetic field are not new (11). One of the most comprehensive investigations of this type was made by R. M. Bozorth and J. F. Dillinger (2). They investigated the nickel-iron and nickel-iron-cobalt alloys. For the nickel-iron alloys Bozorth and Dillinger obtained the greatest increase in maximum permeability at 68% nickel. The highest permeability obtained in their experiments was 600,000. They showed that the effect was obtained only on the cooling part of the annealing cycle below the Curie temperature.

In order to verify the above results we have magnetic annealed the alloys used in the tension annealing investigations. The cooling rate was 85°C/hr. to correspond to that used in tension annealing experiments. Our results obtained on the change in maximum permeability are shown in Plate 18. The highest permeability we obtained was 686,000 occurring at 67.5% nickel. No appreciable change in permeability with magnetic annealing was observed below 50% Ni. It should be noted that at the composition where the magnetostriction is zero (approximately 81% nickel) a substantial increase in permeability was observed. Up to this point, the best results obtained by Bozorth and

PLATE 18

EFFECT ON MAXIMUM PERMEABILITY
OF MAGNETIC ANNEALING
OF NI-Fe ALLOYS



Dillinger have been duplicated. One of the important results of this investigation is that the change in permeability with magnetic annealing actually decreases just below 100% Ni.

In order to investigate the effect of cooling rate on magnetic annealing we have magnetic annealed a set of nickel-iron specimens at a slower cooling rate (15°C/hr.). Our results on the change in maximum permeability are shown in Plate 19. It is seen that the highest maximum permeability is obtained at 60% Ni. This was 1,615,000, the highest ever reported for either polycrystalline or single crystal materials.² Because the cooling rate affected the magnetic characteristics, the rate of cooling was standardized for all magnetic annealing experiments.

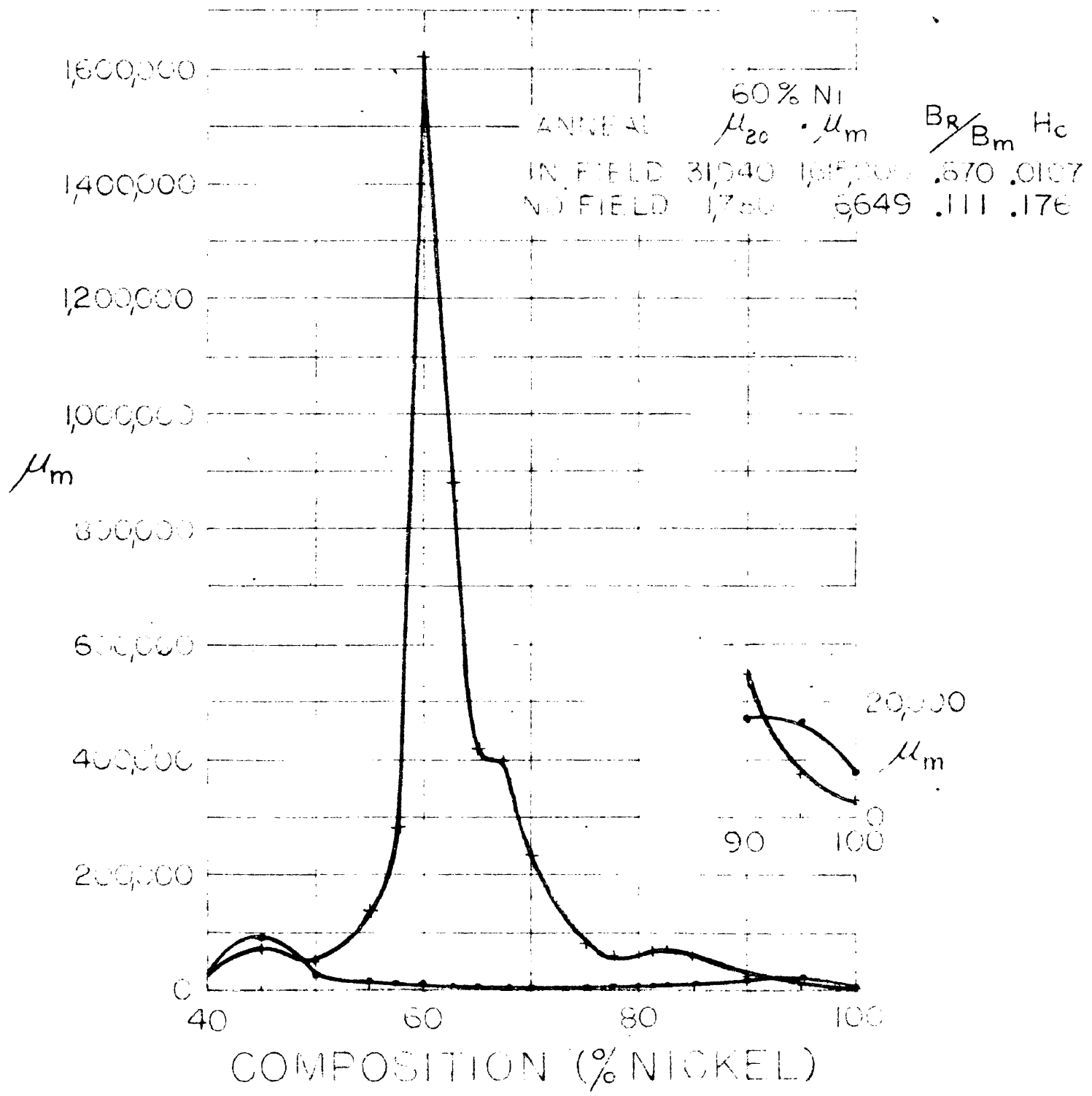
The theory of magnetic annealing proposed by Bozorth and Dillinger is based on the relief of the stresses of magnetostriction by plastic flow at the annealing temperature. Their theory is rather vague. A number of discrepancies in it have already been discussed by Becker and Döring (13). It should be emphasized that magnetization and mechanical forces are coupled together through magnetostriction. Therefore, it is evident why the results of tension annealing should be associated with magnetostriction. However, it is not evident why the changes produced

²The previous record was 1,430,000 for a single crystal of iron established in 1937 (12).

PLATE 19

EFFECT ON MAXIMUM PERMEABILITY (μ_m) OF MAGNETIC ANNEALING Ni-Fe ALLOYS

- + MAGNETIC ANNEAL (FURNACE COOLED IN 87.2 OERSTEDS AT 15°C/HR.)
- NO FIELD (FURNACE COOLED AT 24°C/HR.)



by magnetic annealing should be necessarily associated with magnetostriction. The fact that magnetic annealing produces a substantial increase in permeability when the magnetostriction is zero, seems to contradict the theory. Another discrepancy is that the permeability of nickel decreases after magnetic annealing. The fact that magnetostriction of nickel is negative should make no difference on the basis of the proposed theory. In fact the decrease in permeability does not begin at the composition where the magnetostriction changes sign.

It was decided to investigate the role of magnetostriction by measuring the anisotropy energy introduced by magnetic annealing, f_{MK} . The exact experimental procedure has been described earlier in this report. The cooling rate used was 85°C/hr. Our results are shown in Plate 20 as a function of composition. The new anisotropy energy density is given in terms of a new anisotropy coefficient, K_0 , to be described below.

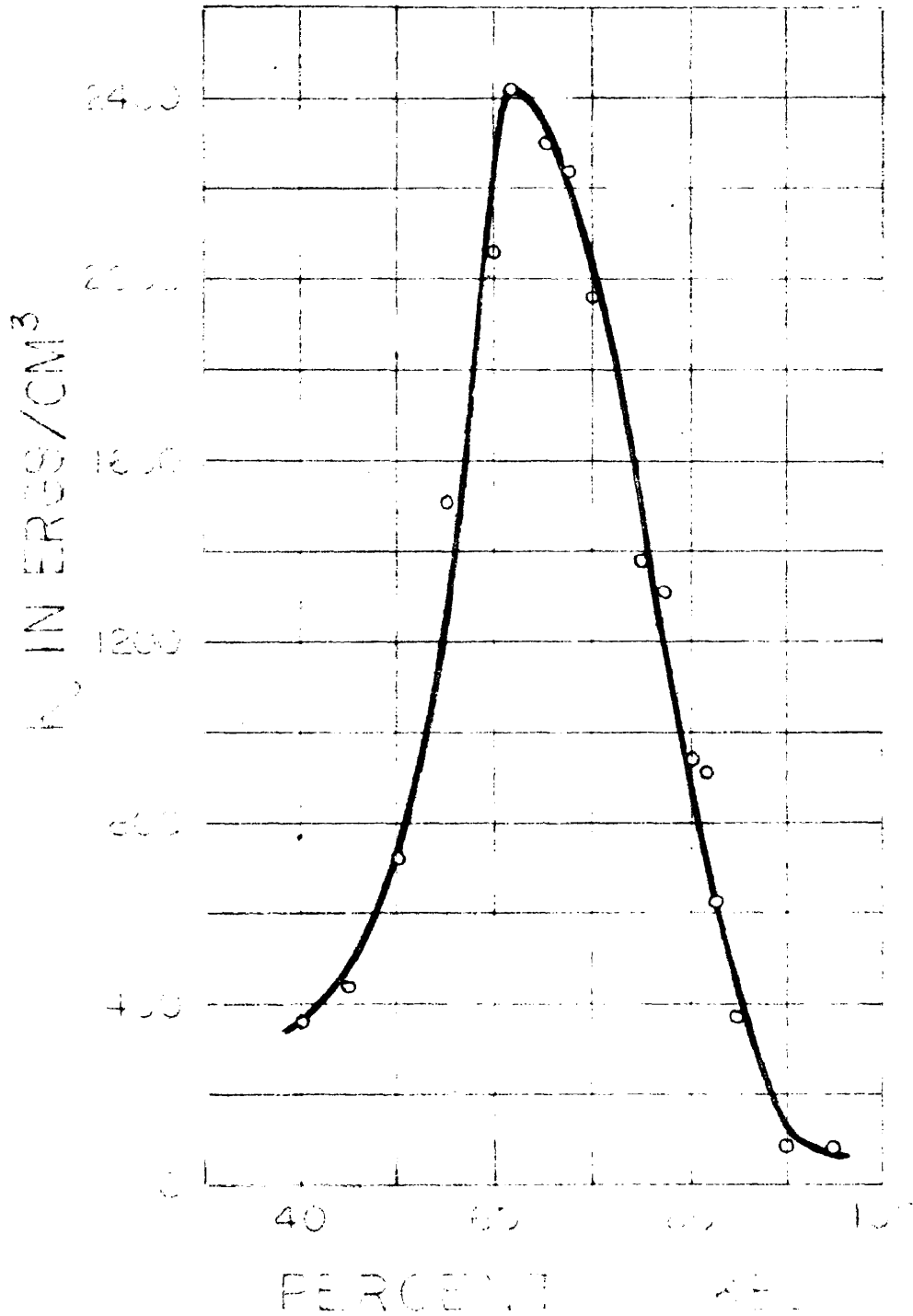
An expression for f_{MK} based on a fixed homogeneous lattice displacement, $\bar{\epsilon}$, is (4)

$$f_{MK} = -3G \bar{\lambda} \bar{\epsilon} \cos^2 \psi$$

where G is the shear modulus of elasticity and ψ is the angle between $\bar{\epsilon}$ and the magnetic field used in measuring the anisotropy. With isotropic magnetostriction there will be a longitudinal extension of magnitude $\bar{\lambda}$ and a lateral contraction of magnitude $\frac{1}{2} \bar{\lambda}$. Since we can neglect volume magnetostriction, this is equivalent to a homogeneous

PLATE 20
 MAGNETIC ANISOTROPY
 CONSTANT K_2
 INTRODUCED BY MAGNETIC ANNEALING

FURNACE COOLED IN FIELD AT $5^\circ\text{C}/\text{HR.}$



displacement $\mathcal{E} = \frac{3}{2} \bar{\lambda}$.

According to the theory under discussion,

$$f_{hk} = -\frac{q}{2} G \bar{\lambda}^2 \cos^2 \psi = -K_0 \cos^2 \psi$$

where K_0 is the new anisotropy coefficient introduced by magnetic annealing.

We will now compare the calculated value of K_0 with the measured value for the 65% nickel alloy. Now $G = \frac{E}{2(1+\sigma)}$ where σ is Poisson's ratio and $\sigma \approx 0.3$ for nickel-iron alloys (14). We may take $\bar{\lambda} = 17 \times 10^{-6}$ and $E = 1.95 \times 10^{12}$ dynes/cm² (14) and obtain K_0 (Calc.) = 925.4 ergs/cc. From Plate 20 we obtain K_0 (Meas.) = 2300 ergs/cc.

According to Becker and Döring (14), at 81% nickel the magnetostriction is zero in all directions and therefore K_0 should be zero. We have found that $K_0 = 800$ ergs/cc at 81% nickel, which is in contradiction to the theory.

Another contradiction to the theory under discussion is the reduction in permeability on magnetic annealing nickel-iron alloys containing more than 92% nickel. If the magnetostriction changed sign at elevated temperatures the discrepancy could be resolved. However, according to Döring's data on the magnetostriction of nickel at different temperatures (6), this does not occur. However, it is known that the anisotropy constant, K_1 , for nickel (5) does change sign as the temperature increases. Now if $K_1 > 0$ during the magnetic anneal, $[100]$ is the "easy" direction of magnetization. The presence of the magnetic field will

result in a torque tending to rotate misaligned domains into the field direction. If this torque can be frozen into the lattice on cooling, somehow, then it might tend to rotate the magnetic vector out of the desired direction where $K_1 < 0$ at room temperature and the "easy" direction changes from $[100]$ to $[111]$.

If the torque tending to rotate the magnetization into the field direction can be frozen into the lattice on cooling, this might account for effects observed on magnetic annealing when $\bar{\lambda}$ is zero. Thus it is possible that a modified form of the plastic flow of domain theory could be retained when $\bar{\lambda} = 0$.

Kaya (15) has proposed that the mechanism of magnetic annealing is associated with superstructure. He suggests that the superstructure acts as a paste and holds the domains in position when the magnetic field is removed. Since pure metals do not form superstructure, this could not explain our results with nickel. The results of magnetic annealing iron have been reported by several investigators. Since their results are conflicting, we have repeated the experiment on two samples of iron. Our results are shown in Table 3. The magnetic ingot iron is of commercial purity and it is seen that only a slight increase in permeability is obtained by magnetic annealing. The electrolytic iron is a purer grade and a significant increase in permeability is obtained. Mihara (16) has carried out similar experiments on silicon-iron alloys. He has found that the presence of

only minute amounts of impurities will suppress the effectiveness of magnetic annealing. Therefore, it is possible that a much greater change in permeability would be obtained if purer iron were used in these experiments.

TABLE III
EFFECT OF MAGNETIC ANNEALING OF IRON

<u>Material</u>	<u>Purity</u>	<u>Maximum Permeability</u>	<u>Final Anneal</u>
Magnetic Ingot Iron	99.89%Fe	8732	Slowly cooled without magnetic field
Magnetic Ingot Iron	"	9266	Slowly cooled in 87.2 oersteds
Electrolytic Iron	99.99%Fe	20,153	Slowly cooled without magnetic field
Electrolytic Iron	"	27,561	Slowly cooled in 87.2 oersteds

However, it is possible that superstructure might be a contributing factor in the mechanism of magnetic annealing of alloys and this will be taken up in the next section.

SECTION VII

SUPERSTRUCTURE

One indirect method of determining the presence of superstructure is by measuring the resistivity of an alloy. This has been done for the alloys used in this investigation using a Kelvin bridge. Our results are shown in Plate 21. The resistivity of the baked specimens deviates considerably from the quenched specimens near 76% nickel. This corresponds to Ni_3Fe .

In order to determine whether the presence of a magnetic field had any influence on superstructure, a quenched specimen was baked for 18-hours at 425°C in a magnetic field. The maximum permeabilities obtained are shown in Plate 22. The dashed curve in Plate 21 shows the resistivities that were obtained. It is seen that we have discovered the significant fact that the formation of the superstructure is retarded by the magnetic field. This is particularly noticeable at 80% nickel and above.

Other experiments were performed in which a baked specimen was re-baked in a magnetic field. It was found that the resistivity increased substantially except when close to the 75% nickel composition where the tendency to form a superstructure was the strongest.

RESISTIVITY OF ANNEALED
 NI-Fe ALLOYS

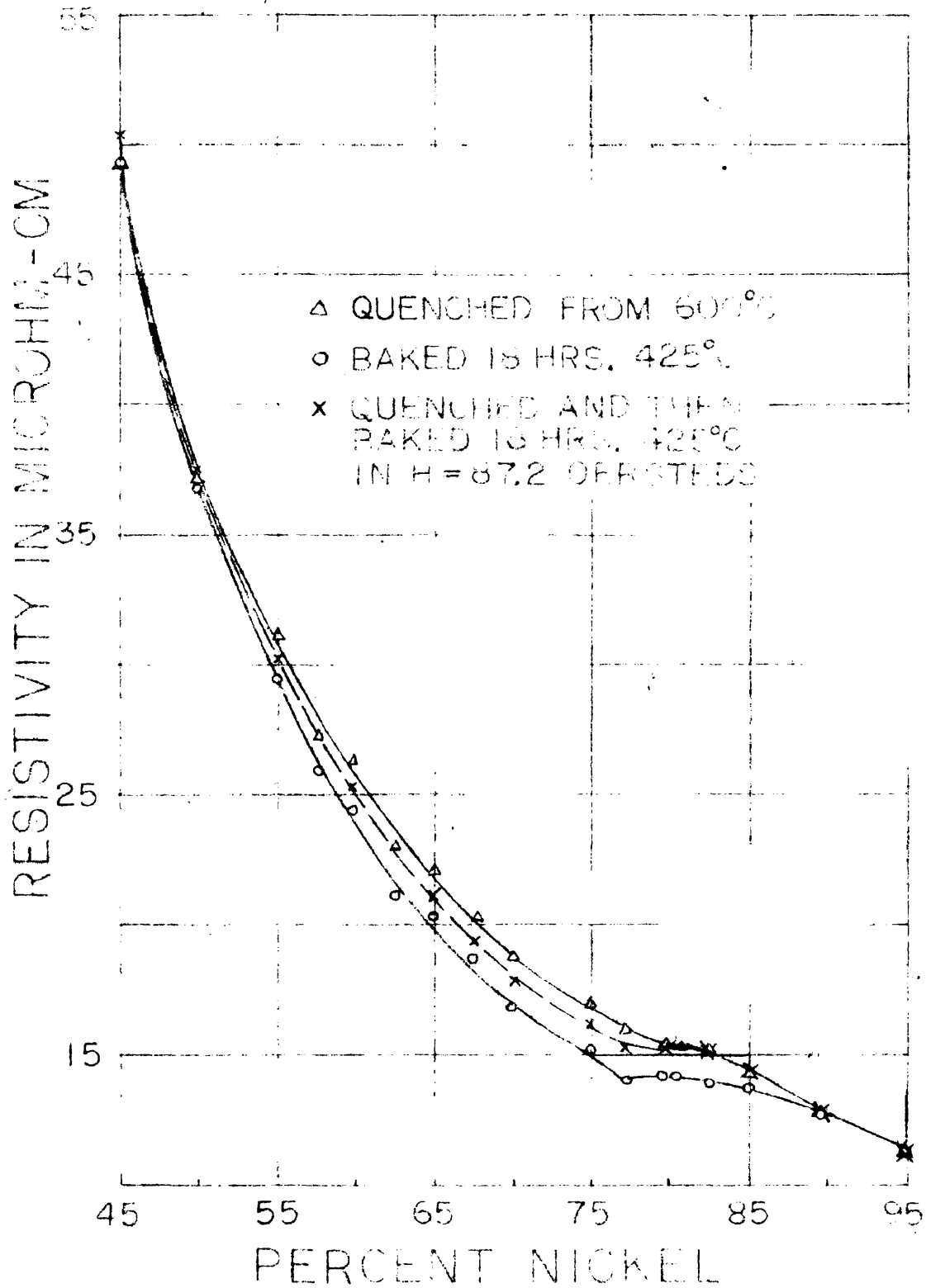
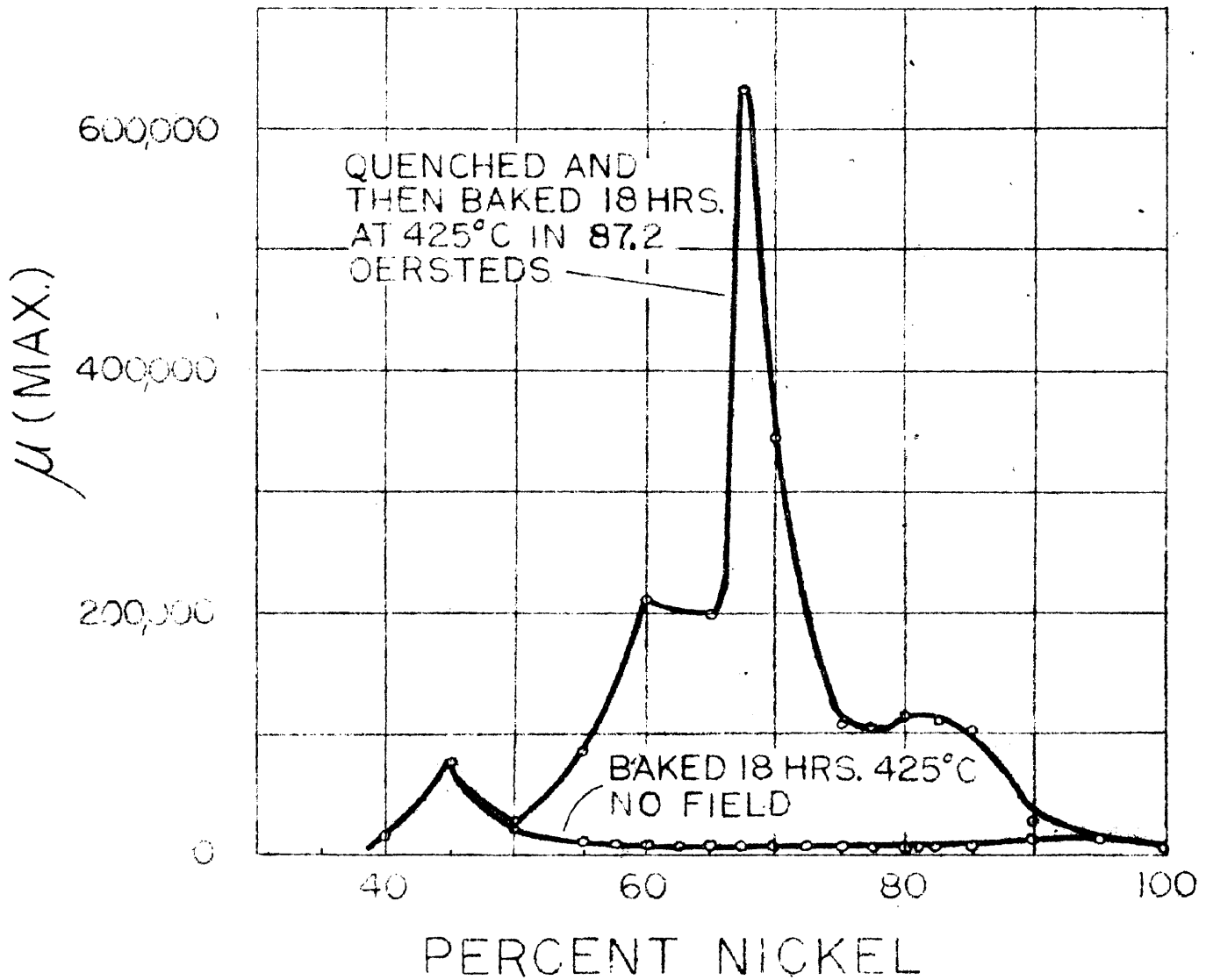


PLATE 22

EFFECT ON MAXIMUM PERMEABILITY
OF BAKED NI-Fe ALLOYS

Thus it is seen that one factor in the mechanism of magnetic annealing is the influence of the magnetic field on the formation of superstructure.

SECTION VIII

BIBLIOGRAPHY OF LITERATURE CITED

- 1 Becker, R. and Döring, W., Ferromagnetismus, Julius Springer 1939, 3411-416.
- 2 Bozorth, R. M., and Dillinger, J. F., Physics 6, Sept. 1935, pp. 279-291.
- 3 _____, Ferromagnetismus, S 281.
- 4 _____, Ferromagnetismus 146.
- 5 Brailsford, P., Magnetic Materials, Methuen & Co., Ltd. 1948, p. 57
- 6 Döring, W., Z.f. Physik, V 103, 1936, pp. 560-582.
- 7 _____, Ferromagnetismus, S 157
- 8 Elmen, G. W., Jr. Franklin Institute, Vol 195 (1923)p.621
- 9 Leech, P., and Sykes, C., Phil. Mag., 1939 Series 7
27, 742
- 10 Becker, R., Wiss. Veroff. Siemens-Werk Bd 11 (1932) S 1
Kersten, M., Z. Techn.Phys. Bd 12 (1931) S 665
- 11 Pender, H., and Jones, R. L., Phys. Rev. 1, 259 (1913)
- 12 Cioffi, P. P.; Williams, H. J.; Bozorth, R. M.,
Phys. Rev., (1937) 51, 1007
- 13 _____, Ferromagnetismus, S 418-
422
- 14 Marsh, J.S., The Alloys of Iron and Nickel, McGraw-Hill, 1938, pp. 109-111
- 15 Kaya, S., Jour. Pac. Sci., Hokkaido Univ., Ser II, Vol 2 (1938) p. 29.
- 16 Mihara, K., Target X-34 (H), NavTechJap Document ND 50-5047